Review | Open Access

Vessel Plus

Du. *Vessel Plus*. 2026;10:62 **DOI:**10.20517/2574-1209.2026.59

Microvascular hyperpermeability and disruption in ischemia-reperfusion: pathophysiology, detection and interventions

Xiao-Jun Du

Keywords:
Ischemia-reperfusion, microvascular damage, microvascular hyperpermeability, inflammation, edema

Citation: Du XJ. Microvascular hyperpermeability and disruption in ischemia-reperfusion: pathophysiology, detection and interventions. *Vessel Plus*. 2026;10:62. https://dx.doi.org/10.20517/2574-1209.2026.59

Received: 30 Jun 2026
First Decision: 25 Aug 2026
Revised: 8 Oct 2026
Accepted: 4 Nov 2026
Published: 23 Nov 2026

Academic Editor:
Frank W. Sellke
Copy Editor:
Fangling Lan
Production Editor:
Fangling Lan

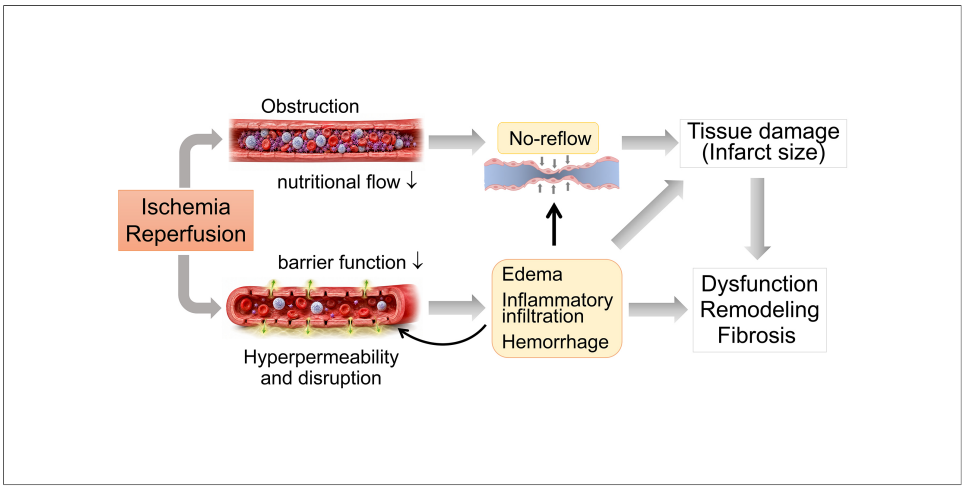

Abstract

Ischemia-reperfusion (IR) is commonly seen in a variety of clinical conditions and affects multiple organs. For a long time, drug and non-drug therapies have focused on the salvage of primary functional cell types of a jeopardized organ. Current therapies are able to ameliorate the degree of organ damage, limit the infarct size, and reduce mortality. However, the efficacy is not optimal, as judged by the inadequacy in preventing chronic adverse organ remodeling and functional preservation. Composed of endothelial cells, microvasculature is a key supportive structure vital for normal organ function but vulnerable to IR insult. Microvascular damage (MVD) exhibits multifaceted features, including microvascular hyperpermeability (MVHP), which is manifested as tissue edema, inflammatory infiltration, and microvascular disruption leading to tissue hemorrhage, and has been increasingly appreciated as a pivotal event that impacts the degree of organ IR injury. In the setting of IR, there has been no effective therapy for MVD, particularly for MVHP. This review discusses features of MVHP and its pathophysiology, explores research techniques for the detection of MVHP, and summarizes preclinical findings on therapeutic interventions. At the end, I highlight the significance of the loss of endothelial barrier function in clinical settings of cardiac and brain ischemia and suggest future research directions.

Experimental Cardiology, Baker Heart and Diabetes Institute, Melbourne 3004, Australia.

Correspondence to: Dr. Xiao-Jun Du, Experimental Cardiology, Baker Heart and Diabetes Institute, 75 Commercial Road, Melbourne 3004, Australia. E-mail: xiao-jun.du@baker.edu.au

INTRODUCTION

Ischemia-reperfusion injury (IRI) frequently occurs in a range of clinical conditions that involve multiple organs. The most common clinical conditions are cardiac and brain ischemia caused by atherothrombosis of coronary or cerebral arteries. Organ transplantation is another condition where a transplanted organ, e.g., the heart, lungs, kidney, liver, or intestines, undergoes a significant period of ischemia followed by restoration of blood circulation. Under conditions of cardiopulmonary bypass surgery, cardiogenic, hemorrhagic, or septic shock, or resuscitation of cardiac arrest, multiple organs may undergo IRI. Regional embolism of pulmonary, intestinal, or limb arteries may also cause IRI of corresponding organs.

Timely restoration of blood flow in settings of cardiac and cerebral ischemia has become a therapeutic routine in the clinic to limit organ damage. However, the development of IRI constitutes a major hurdle to this clinical goal. IRI has long been recognized in the clinic, but effective treatment remains to be developed. In addition to damage to primary organ cell types like cardiomyocytes or neurons, the microvasculature also represents a key cellular component in the development of overall organ IRI. Our concept of organ IRI has evolved from the damage to the main functional cell type to an appreciation of the significance of damage to supportive cell types, particularly microvasculature[1-5]. Preclinical studies have indicated that, in addition to limiting the infarct size, interventions targeting microvascular damage (MVD) are able to preserve organ structure and function (for review, see[1,6-9]). Hence, there has been a strong momentum of extending therapeutic interventions of IRI toward targeting MVD, as well as preservation of organ structure and function. Microvascular obstruction (MVO), i.e., the no-reflow phenomenon, has been a topic of numerous review articles[3,5,10-15]. Another key function of microvasculature is forming a physical barrier between blood circulation and tissues, through which plasma proteins, ions, and even water pass through the single-layered capillary wall in a tightly controlled manner. Being pivotal to tissue health, the barrier function of microvasculature is governed by intercellular junctions, through which microvessels determine the size of the extracellular volume[16-19]. Current research has demonstrated that this barrier function of microvasculature is lost from the very early phase of ischemia-reperfusion (IR). This review focuses on microvascular hyperpermeability (MVHP) and MV disruption, which form a key component of MVD and significantly impact the overall IRI of organs. The pathophysiological features, current understanding of the mechanisms, methodologies for detecting MVHP, and recent preclinical findings on therapeutic interventions are discussed. The potential translational barriers and key questions in future research will be addressed at the end. In addition to referring to studies on cardiac IRI, this review also refers to many recent publications in the field of ischemic stroke, in which MVHP, more specifically blood-brain barrier (BBB) disruption, has a significant impact on clinical outcomes and therefore is regarded as a pivotal therapeutic target. As discussed, the substantial amount of research findings on MVHP in ischemic stroke enrich our knowledge and are potentially applicable to mechanistic and therapeutic research on cardiac IRI.

MULTIFACETED FEATURES OF MVD AND CONSEQUENCES OF MICROVASCULAR HYPERPERMEABILITY

Forming the interface between circulating blood and tissues, microvascular units play two fundamental functions: supplying tissues with nutritional blood flow and maintaining tissue homeostasis[1,8]. Microvasculature is composed of a single layer of endothelial cells (ECs) that are equally vulnerable to IRI compared with cardiomyocytes or neurons as primary organ cell types, given that MV abnormalities occur very early after IR[2]. IR evokes diverse alterations of microvasculature, including augmented reactive oxygen species (ROS), enhanced adhesion to circulating leukocytes or platelets, loss of the barrier function, or even further damage leading to capillary disruption or formation of microthrombosis [Figure 1][1,5]. During this dynamic process, ECs initially undergo pro-inflammatory phenotype-switching driven by reversible events including blood cell-EC interactions, augmented ROS, mitochondrial dysfunction, and Ca^{2+} overload.

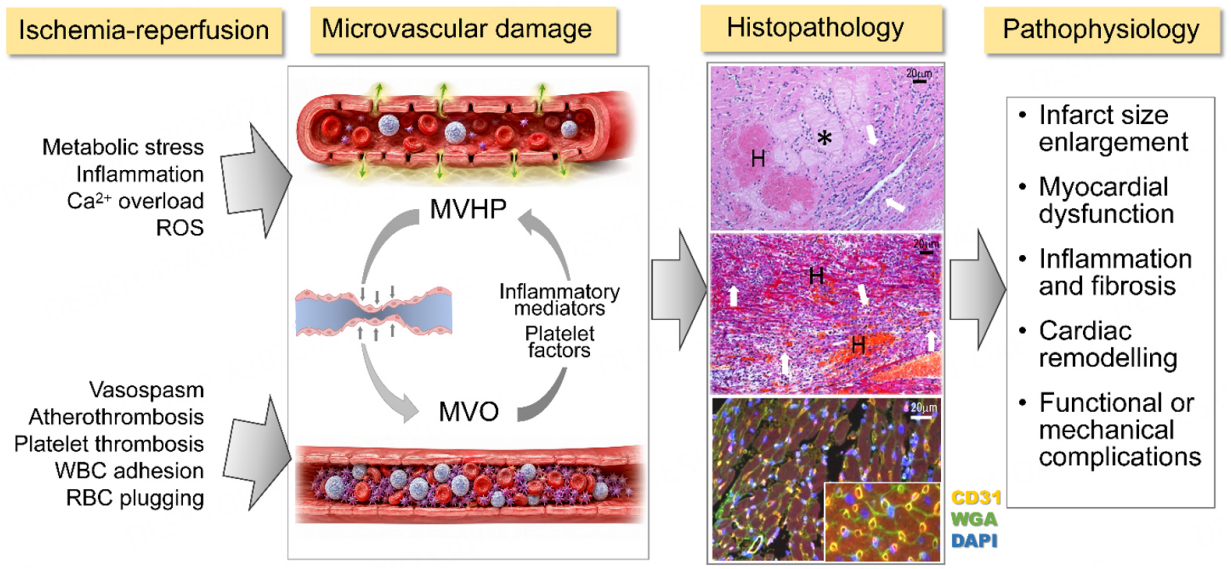

Figure 1. Microvascular damage (MVD) constitutes a pivotal component of ischemia-reperfusion (IR) and contributes to the development of IR-induced organ damage, dysfunction, and subsequent remodeling. IR-associated MVD represents not only microvascular obstruction (MVO) with impaired tissue perfusion (no-reflow), but also microvascular hyperpermeability (MVHP) or disruption. MVHP exacerbates tissue edema, inflammatory infiltration, tissue hemorrhage, and MVO. WBC, white blood cells; RBC, red blood cells. Cardiac histological images from mice subjected to IR reveal tissue edema (*), hemorrhage (H), inflammatory infiltration (white arrows), and a closed capillary lumen compared with the control heart (inset). The vascular diagrams were created using an AI-powered text-to-visualization tool (PicDoc beta version; https://www.picdoc.cn).

Further progression of MVD occurs as a consequence of cell death and structural disruption that exacerbate microvessel leakage with blood cell extravasation and tissue hemorrhage [Figure 1][5,20]. Clinically, cardiac magnetic resonance imaging (MRI) studies have revealed the occurrence in about 35%-55% of patients with ST-segment elevation MI (STEMI) of myocardial edema and eventually intramyocardial hemorrhage (IMH), and that the presence of these cardiac MRI signs is accompanied by adverse clinical outcomes independent of MVO[21-27].

In organs subjected to IR, MVD occurs as a chain of events involving inflammatory phenotypic switching of ECs, reduced nutritional blood flow, MVO, MVHP, or structural disruption, resulting in tissue edema, inflammatory infiltration, and hemorrhage. All these contribute significantly to short- and long-term organ damage and dysfunction [Figure 1]. In cardiac IR, ischemia and inflammation are known to disintegrate endothelial junctions through intracellular signaling, resulting in the onset of MVHP[2]. Whereas MVO and MVHP are closely related events in the setting of IRI, there has been increasing appreciation of potentially distinct mechanisms responsible for MVO (blockade from inside)[5,10,12] and MVHP/MV disruption[1,4,23,27]. Animal studies have well established the timeline for the development of MVO or infarct following IR. In the mouse, myocardial infarct does not occur if an ischemic episode is brief (under 15 min)[28]. Using Evans blue as an indicator in an MV permeability assay, we found in mice that MVHP is detectable within 15 min of ischemia and becomes more severe with a more prolonged ischemic period [Figure 2A]. Further, following cardiac IR (1/24 h), the size of the jeopardized myocardium exhibiting MVHP is twice as big as that with MVO and also significantly larger than the infarct size [Figure 2B][2]. As discussed below, mechanistically, MVO is mainly due to blockade within the vessel lumen for reasons including atherothrombotic embolism, microthrombosis, and inflammatory cell adhesion to the surface of jeopardized ECs [Figure 1]. At the same time, disintegration of EC tight junctions (TJ) and adherens junctions (AJ) and MV disruption are critical for the onset of MVHP. Importantly, tissue edema, inflammation, or hemorrhage due to MVHP and MV disruption exacerbate MVO by compressing capillaries [Figure 1] externally.

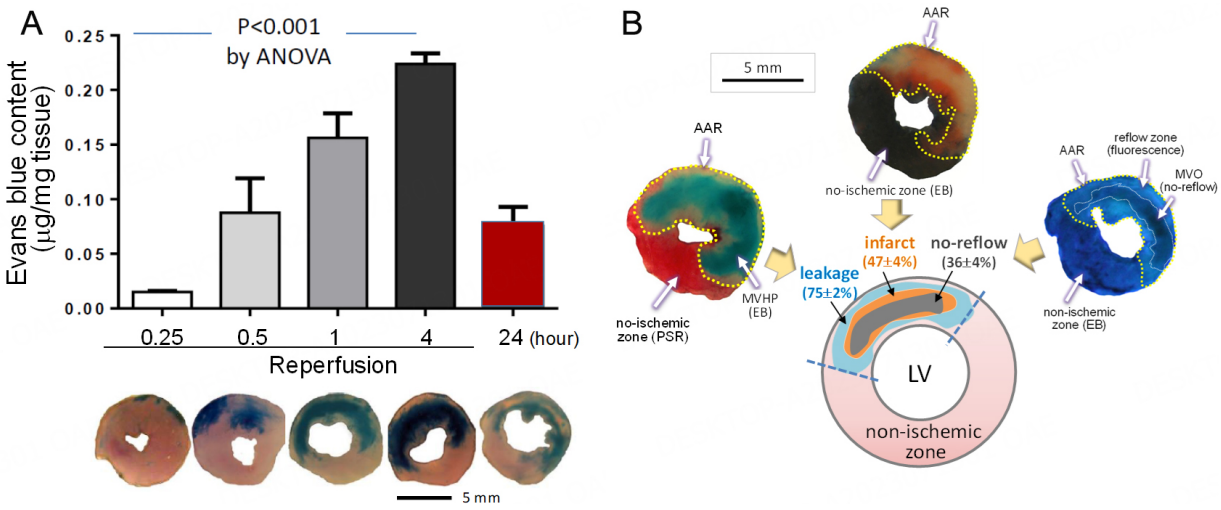

Figure 2. Features of MVHP in the mouse heart subjected to IR. (A) Chromatographic determination of tissue content of Evans blue showing that the severity of MVHP in the ischemic myocardium is ischemic duration-dependent. The data were obtained from mice subjected to coronary artery occlusion of varying periods followed by reperfusion up to 24 h. For comparison, tissues from mice with 24-h permanent ischemia without reperfusion were also analyzed. Also shown are representative histological images of left ventricular (LV) sections with regions of MVHP stained by Evans blue (EB). Data are mean ± SEM, n = 5 per group. (B) Determination of LV zones of MVHP, infarct, or microvascular obstruction (MVO) by dual-staining methods in the mouse heart subjected to IR (1/24 h). Histological images of LV sections show MVHP stained by intravenously injected EB plus intracoronary injection with picro-sirius red (PSR, indicating the area-at-risk indicated by the yellow dotted line). The necrotic myocardium is ascertained by the absence of triphenyltetrazolium chloride (TTC) staining (pale color) within the area-at-risk (AAR) and the non-infarct zone stained dark blue by intracoronary injection with EB after re-occlusion of the left coronary artery. MVO is shown by the absence of thioflavin-S fluorescence (indicated by a fine white dotted line) within the AAR, and the non-infarct zone by EB injected via aortic cannulation. The results were derived from 10-12 hearts per parameter. Using these staining methods and normalization by the AAR, the size of the myocardium exhibiting MVHP (leakage) is significantly larger than the size of the infarct or MVO. Adapted with permission from Ref.[2], Copyright © 2017 by American Physiological Society.

MECHANISMS RESPONSIBLE FOR MICROVASCULAR HYPERPERMEABILITY

Dynamic evolution of MV leakage following IRI

IR-induced MVD can be regarded as a dynamically and rapidly evolving chain of events. Capillaries might be "blockade-from-inside", leading to sluggish or blocked blood flow by factors including inflammatory cell adhesion, EC swelling, red blood cell packing, atherothrombotic debris, and microthrombosis[5]. Meanwhile, the EC wall becomes hyper-permeable (leakage), facilitating extravasation of water, ions, and protein into the interstitium, forming edema, which compresses capillaries externally, contributing to MVO by "blockade-from-outside" [Figure 1]. A more severe form of MV leakage can occur following EC death and capillary disruption with resultant hemorrhage, in particular IMH [Figure 3A-C][21,22,25]. In fact, IMH together with dense infiltration of inflammatory cells and regional accumulation of platelets is a common histological sign in the infarct myocardium of human patients[21,22,25,29,30] or mice[31,32]. MVHP is initially the consequence of functional abnormalities of ECs, but subsequently involves irreversible structural damage. Current research indicates that several molecular and cellular mechanisms are involved in the development and progression of MVHP [Figure 3]. MVHP following IR is initially a regulated and reversible process involving numerous signaling changes. However, with the progression of IRI, MVHP evolves into irreversible processes characterized by EC death and MV structural disintegration [Figure 3C]. It remains unclear what process is required for the onset of irreversible MV disruption. Given that the prevalence of cardiac MRI-IMH in patients is higher in days 3-7 post-STEMI, it is tempting to speculate that the peak time for irreversible MV disruption occurs in patients around day 4[21,23,25].

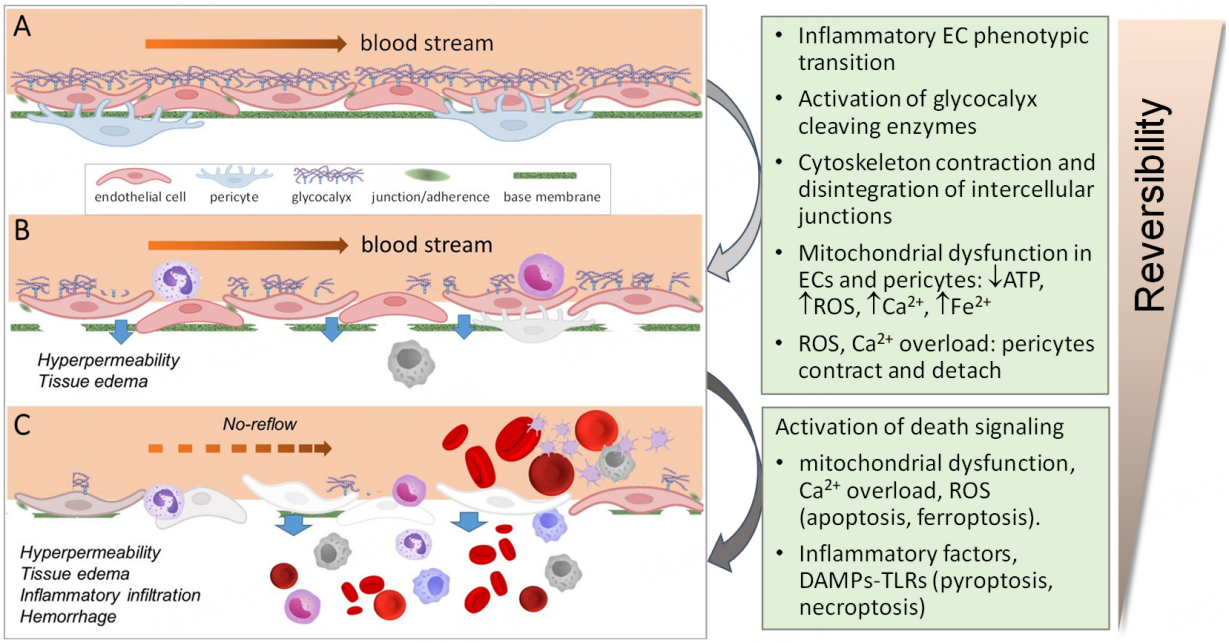

Figure 3. Dynamic evolution of MVHP and disruption in IRI. (A) MV barrier function is based on intercellular tight junctions and adherens junctions, and further reinforced by out-surface localized pericytes and the basement membrane, and an inner-surface layer of glycocalyx. (B) Following IR, metabolic disturbances in EC, increased inflammatory stimuli, accumulation of reactive oxygen species (ROS), and Ca^{2+} evoke contraction of cytoskeletal filaments, leading to splitting of intercellular junctions and the onset of MVHP. Other critical changes at this stage include damage and shedding of the glycocalyx layer and inflammatory phenotypic changes in ECs, including expression of adhesion molecules, which facilitate adhesion, rolling, and extravasation of circulating inflammatory cells. (C) Further worsening of damage to MV results in MV structural disintegration following EC and pericyte death or pericyte detachment and degradation of the base membrane. Tissue edema and blood cell extravasation could exacerbate no-reflow through compressing capillaries. Text boxes on the right indicate, in chronological order, key signaling mechanisms pivotal in mediating reversible MVHP and irreversible MV disruption. Blood cell images were from online Pixabay Free Blood Cells Images (https://pixabay.com).

Microvascular inflammation

IRI rapidly triggers inflammation that becomes increasingly severe, driven by factors such as cytokines, chemokines, danger-associated molecular patterns, and interactions between immune cells and microvascular ECs at the inner surface. Contributing to the regional inflammation also involves the inflammatory phenotypic switching of ECs, characterized by the enhanced expression and surface localization of intercellular adhesion molecule and vascular cell adhesion molecule[33]. These adhesion molecules participate in immune cell anchoring, rolling, and infiltration [Figure 3B and C][32]. In the next stage, microvascular ECs undergo cell death together with basement membrane damage and pericyte dysfunction or detachment, changes synergistically leading to structural disruption with resultant hemorrhage and massive inflammatory infiltration together with platelet extravasation [Figure 3C][32,34]. Importantly, tissue edema and regional inflammation exacerbate regional "no-reflow" phenomenon and tissue injury [Figure 1][2].

Damage to endothelial glycocalyx

The luminal surface of ECs is covered by a layer of glycocalyx formed by cross-linked glycoconjugates like glycolipids and glycoproteins that are anchored to transmembrane domains or membrane structural phospholipids of ECs. The glycocalyx structure is hydrophilic, with viscous and gel-like properties through which the glycocalyx provides a buffer between ECs and blood circulation, and contributes to the maintenance of MV health and barrier function, EC mechanotransduction, and regulation of nitric oxide (NO) production[35,36]. Studies have found that under IR or simulated conditions, endothelial glycocalyx structure is degraded and becomes thinner and spacer with glycocalyx coat shedding into the

circulation[35,37-39]. The mechanism of endothelial glycocalyx damage during IR remains partially understood, and several enzymes are known to be activated, cleaving the glycocalyx at different sites. While matrix metalloproteinases (MMPs) cleave proteoglycans (e.g., syndecan-1) directly from the EC membrane, heparanase cleaves the heparan sulfate chains attached to core proteoglycans, and hyaluronidase degrades the hyaluronan [Figure 3]. Regional ROS, inflammatory mediators, thrombin, and the complement system facilitate glycocalyx degradation[35,38,40-44]. In the mouse brain IRI model, elevated BBB permeability occurs together with regional accumulation of hyaluronidase activity and disruption of the glycocalyx, which involves enhanced interaction between syndecan-1 and Src, leading to remodeling of cytoskeletal proteins and augmented endocytosis[45]. Glycocalyx shedding into the circulation holds the potential to become biomarkers of MVHP, including hyaluronan and syndecan-1 as major components of the glycocalyx[44,46]. In renal ischemic or non-ischemic diseases, damage to the glycocalyx of ECs has been shown to contribute to proteinuria[6,47,48].

Endothelial metabolic dysfunction

Mitochondrial metabolism and ROS levels are involved in cellular signaling in response to environmental alterations and play a crucial role in the maintenance of MV function, and abnormalities of EC mitochondria contribute significantly to IR-associated MVHP[49-51]. Mitochondrial dysfunction in ECs causes a chain of events such as adenosine triphosphate deficiency, oxidative stress, endoplasmic reticulum stress, intracellular Ca^{2+} overload, and eventually programmed cell death, leading to MVHP and MV disruption[49-52] [Figure 3]. Intracellular Ca^{2+} accumulation in ECs and pericytes has been shown to be closely related to mitochondrial dysfunction and ROS accumulation[53].

Disruption of intercellular junctions

The integrity of the endothelial barrier is controlled by intercellular contact complexes of AJ and TJ. Adherens junctions consist of E-cadherin, -catenin, and platelet-endothelial cell adhesion molecule 1, while TJ are formed by occludins, claudins, and junctional adhesion molecules. These proteins are anchored to actin cytoskeleton filaments of EC via catenins (or p120 isoforms) for AJs or by zona occludens proteins for TJs. Under IRI stimuli, phosphorylation of myosin light chain (MLC) drives cross-bridge cycling of myosin and actin that induces actin cytoskeletal contraction and disruption of AJs and TJs[33,54]. Several factors mediate disruption of the junctional complexes leading to MVHP, in which inflammatory stimuli are regarded as the most potent signaling. Inflammatory mediators, including histamine, vascular endothelial growth factor (VEGF), thrombin, or immune cell-EC interactions, activate respective membrane receptors and intercellular signaling pathways, resulting in dissociation of the junctions, an effect amplified by EC inflammatory phenotypic transition and intracellular Ca^{2+} overload[55-58]. Studies have implicated that activation of several kinases, including Rho kinase[59], phosphatidylinositol 3-Kinase[60,61], or MLC kinase[62], weakens the specialized junctions, leading to MVHP. Disruption of EC junctions is also central to MVHP onset in other organs subjected to IRI[56,63-66]. There is strong evidence from studies on ischemic stroke that extravascular exposure of red blood cells per se, either lysate, hemoglobin, hemin, Fe^{2+}, or whole cells, induces BBB disruption[19,53]. Similarly, intravenously administered platelet-derived factors also induce MVHP in the lungs[67]. Sphingosine-1-phosphate (S1P)/S1P receptor 1 (S1PR1) signaling maintains MV function. Zhao *et al.* reported that EC-restricted deletion of S1PR1 promotes MVHP of the coronary microvasculature under brief IR or acute pressure-overload stress through mechanisms involving intracellular Ca^{2+} accumulation, enhanced MLC phosphorylation, and actin cytoskeletal contraction[68].

Dysfunction or depletion of pericytes

Pericytes form a coat over the external surface of microvasculature, with a degree of coverage from 20% to 80% depending on organs[69-71]. There exist close interactions between pericytes and ECs, both structurally via adhesions, nanotubes, and peg-socket structures, and functionally through molecules including integrins and

multiple receptors (e.g., vascular endothelial growth factor receptor, VEGFR, and Notch-Jagged1, S1PR1) expressed in both cell types[69,71,72]. Through several signaling pathways, mutual communication between pericytes and ECs jointly regulates cellular turnover and function, in particular, nutritional blood flow and permeability [Figure 3][53,69,71,73]. However, activated pericytes express and release cytokines and hypoxia-inducible factor-1 (HIF-1) that act on adjacent ECs, contributing to the onset of MVHP[69,71,72]. Brain pericytes play a crucial role in the maintenance of the BBB and post-IR restoration of barrier function[70,74]. Using the ischemic stroke model, Roth *et al.* showed that pericytes are more vulnerable than ECs to IRI, with contraction, cell death, and detachment occurring in less than one hour post-IR[70]. Under IRI, higher levels of intracellular Ca^{2+} and ROS provoke contraction of pericytes that contributes to sluggish blood flow or no-reflow[75]. Pericytes usually die of apoptosis or detach from microvessels soon after contraction[69,76].

Integrated signaling mechanisms for MVHP and irreversible MV disruption

Pro-MVHP signaling is complex and derived from external (inflammatory signaling, bioactive factors, hypoxia) and intracellular (mitochondrial dysfunction, ROS, Ca^{2+} overload, and receptor-mediated signaling in ECs or pericytes) mechanisms [Figure 3B]. Platelet-activating factor (PAF) or bacterial toxin given intravenously induced a rapid onset of pulmonary MVHP occurring within 10 min after administration and progressively worsening[67]. This inflammatory mechanism may explain the finding that following IR in one organ, MVHP could occur in remote organs[77-82]. Importantly, MVHP and inflammation mutually promote each other, forming a vicious cycle[26,33,83]. One strong piece of evidence for MVHP as a hallmark of inflammation is that inflammatory stimuli, such as endotoxins or inflammatory cytokines, are able to induce rapid onset of MVHP when tested *in vitro* and *in vivo*[68,84-88]. In cultured EC monolayers, treatment with tumor necrosis factor-α (TNF-α) or lipopolysaccharide leads to hyperpermeability[68]. Thus, there is strong evidence from *in vivo* studies that single proinflammatory factors are sufficient to trigger MVHP *in vitro* or *in vivo*[33,68,85,86,88]. On the other hand, several studies on buffer-perfused hearts indicate that, in the absence of blood cells, IR per se is able to induce MVHP (vide infra), suggesting a causal role of factors, such as metabolic stress and enhanced ROS, in inducing MVHP[42,55,57,89,90]. Nevertheless, in the setting of IRI, all these factors operate synergistically and sequentially in inducing reversible MVHP followed by irreversible MV disruption [Figure 3C].

A few signaling pathways are found to be protective against MVHP, including S1PR1, insulin-like growth factor-1 (IGF-1), HIF-2, and exchange protein directly activated by cAMP (Epac). S1P/S1PR1 signaling plays an important role in maintenance of hemostasis and barrier function in ECs, and EC-specific deletion of S1PR1 substantially exacerbates EC dysfunction when studied under conditions of IRI in the brain and the heart[68,91]. In cultured human brain microvascular ECs, hypoxia-induced MVHP was prevented by treatment with thymosin-4 through activation of S1PR1[92]. This observation is in keeping with our *in vivo* finding in mice with EC-specific S1PR1 knockout, showing that MVHP induced by IR (15 min/24 h) was exacerbated[68]. The IGF-1 signaling is protective against MVHP in the heart with IRI[93]. NO generated by endothelial nitric oxide synthase (eNOS) can activate cAMP/Epac signaling, thereby preserving EC barrier dysfunction even in the presence of continuous inflammatory stimuli[33,94]. HIF-2 signaling is protective against MVHP in IRI of the lungs or the heart[95,96]. Activation of several kinases has been shown to contribute to MVHP in the setting of organ IRI or simulated conditions, and that specific kinase inhibitors reduce organ MVHP, including ML-7 for myosin light chain kinase in skin MVHP induced by trauma or sepsis-inflammation[62], PF-573228 for focal adhesion kinase in intestine IRI model[97], Imatinib for tyrosine kinase in rat cardiac IRI model[90], sevoflurane or Y-27632 for RhoA in pulmonary or brain IRI models[59,86], and FRAX486 or IPA-3 for p21 activated kinase1 in the stroke model [Table 1][98].

Table 1. Preclinical studies on therapeutic interventions with results showing ameliorated MVHP in perfused heart or *in vivo* models of cardiac or brain IR

Drugs tested	Actions	Organ subjected to IR	Reference
Nisoldipine, Verapamil	Ca^{2+} channel blockade	Perfused heart (rat, 15 or 30 min); drug given before ischemia	[55,57]
Bendavia (mitochondria-targeted peptide)	Reducing ROS, infarct volume, and BBB disruption	Brain (mouse, MCAO 2/24 h); drug given i.v. after reperfusion	[129]
Relaxin	anti-inflammation, preservation of VE-cadherin	Heart (mouse, IR 1/24-48 h); drug given i.p. after ischemia	[85]
CU06-1004	Inhibiting EC inflammatory signaling and cell death	Heart (rat, 30 min/24 h); drug given i.v. prior to reperfusion	[128]
Imatinib	Tyrosine-kinase inhibitor	Heart (rat, IR 45 min/3 h; or perfused heart 40 min/2 h); drug given i.v. prior to ischemia	[90]
Losartan	Blocking AT1R, inhibiting Arc activity, inflammation, and limiting infarct size	Heart (mouse, IR, 1/24 h); drug given i.p. upon reperfusion	[126]
TRPV4 blockers (HC067047, GSK2193874)	inhibiting Ca^{2+} entry in EC with anti-inflammatory and infarct size	Heart (mouse, IR 1/24 h) Brain (mouse, MCAO 45 min/24 h), drug given i.p. upon reperfusion	[58,105]
Methylene blue	Inhibiting Aquaporin 4	Brain (rat, MCAO 1/48 h); drug given i.v. after reperfusion	[130]
Sac-1004	BBB stabilization and anti-inflammatory effects	Brain (rat, MCAO 2 h ischemia), drug given i.v. 30 min after ischemia	[143]
EphA4-Fc (EphA4 inhibitor)	Inhibiting EC contraction and preserving BBB integrity	Brain (mouse, MCAO 1 h), drug given i.p. 1 h before ischemia	[132]
Normobaric O_2 (NBO, 40%)	MV protective via activation of Nrf2	Brain (mouse, MCAO, 1.5/24 h); NBO commenced from ischemia	[127]
miR-383-5p	Likely inhibiting NOX4 expression	Brain (rat, MCAO 5 h); drug given i.v. during ischemia	[144]
Y-27632	Inhibiting ROCK1/MLC-NMMHC interaction to stabilize EC cytoskeleton	Brain (mouse, MCAO, 1/24 h); drug given i.v. 1 h after reperfusion	[133]
SYS18 (1,2,4-Triazole derivative)	Anti-ROS and preventing glycocalyx degradation	Brain (mouse, MCAO, 1/24 or 48 h); drug given i.p. prior to reperfusion	[140]
JNJ0966 + BI-0115	Joint inhibition of MMP-9 and LOX1	Brain (rat, thrombin stroke model); drugs given i.v. 4 h post ischemia	[145]
Verteporfin	Inhibiting YAP activity	Brain (mouse, MCAO 1/24 h); drug given i.p. before reperfusion	[76]
CYM-5442, FTY720	Activating S1PR1 signaling	Brain (mouse, MCAO, 35-90 min); drugs given i.p. during ischemia	[91]
A@HPB@THSA, biomimetic nanozyme	Brain-targeted, ROS scavenger, antiplatelet and anti-inflammatory	Brain (rat, 1.5/24 h), drug given i.v. before reperfusion	[146]

Arc: Activity-regulated cytoskeleton-associated protein; AT1R: angiotensin II type-1 receptor; MMP: matrix metalloproteinase; NMMHC: non-muscle myosin heavy chain; NOX4: NADPH oxidase 4; Nrf2: nuclear factor erythroid 2-related factor 2; MCAO: middle cerebral artery occlusion; ROCK1: Rho-associated: coiled-coil-containing protein kinase 1; ROS: reactive oxygen species; S1PR1: sphingosine-1-phosphate（S1P) receptor1; YAP: yes-associated protein; VE: vascular endothelial.

LABORATORY AND CLINICAL DETECTION OF MVHP AND MV DISRUPTION

Tissue edema mainly involves extracellular (or vasogenic, interstitial) edema, with fluid and plasma proteins leaking into the interstitial space, and is a sign of MVHP. Intracellular (cytotoxic) edema due to energy deficiency might also present in organ IRI. However, the vasogenic edema is likely the predominant form given the co-existence of tissue edema and the loss of EC barrier function evidenced by findings using either permeability tracers (like Evans blue, fluorescent molecules) or imaging contrasts (gadolinium contrasts for MRI or iodine for dual-energy computed tomography [CT])[2,99-103]. Currently, MRI and CT are valuable techniques for *in vivo* detection of tissue abnormalities as a consequence of MVHP and MV disruption leading to edema or hemorrhage. Experimentally, several techniques are useful in detecting the presence of tissue edema and, more importantly, MVHP.

Myocardial edema by routine histology

Histologically, post-infarct myocardial vasogenic edema is characterized by frothy fluid or myoxid-like changes between myocytes, either dead or alive. It is also common to see separation of myofibrils and muscle bundles by expanded interstitial spaces filled with pale-pink material, as well as inflammatory infiltration, depending on the duration of IRI [Figure 1]. In ischemic stroke, brain edema appears mainly in the white matter and perivascular regions with separation of myelinated nerve fibers. This histological method provides only a non-quantitative observation of tissue edema with unpredictable results depending greatly on the regions examined. Therefore, this measure is unable to become routine, and its use in clinical studies is significantly impeded due to the difficulty of obtaining human tissue samples.

Desiccation for tissue edema

The severity of tissue edema can be measured in harvested tissues using the dry-wet method. After recording wet weight (W_{Wet}), the tissue sample is treated either by freeze-drying or vacuum-drying to complete dryness, ascertained by a stable reading of dry weight (W_{Dry}). The water content in the tissue sample is calculated from the difference between W_{Wet} and W_{Dry}, and fractional tissue water content is derived by: $[(W_{Wet} - W_{Dry})/W_{Wet}] \times 100\%$. While providing a quantitative measure of edema, the drawbacks of this method are the requirement of freshly harvested tissue and tissue consumption; therefore, it is limited to laboratory research only. Currently, quantifying tissue water content *in vivo* represents a major technical challenge.

Hyperpermeability tracer-aided histology

In animals subjected to cardiac IRI, we showed that Evans blue dye [Figures 2, 4, 5A] or IRDye-800CW [Figure 5B], injected intravenously 3 h prior to heart collection, is able to stain the myocardium with MVHP. The heart needs to be thoroughly washed through an aortic cannula to remove remaining tracer-containing blood in the coronary vascular bed. Both tracers have strong affinity for circulating proteins, and tracer extravasation indicates MVHP. fluorescein isothiocyanate (FITC)-conjugated albumin can also be used. The passage of fluid and a tracer across the microvascular wall is determined by the hydrostatic-osmotic pressure gradients across the EC barrier and the barrier's properties. The amount of a tracer that crosses the EC per unit time (J_{tracer}) is determined by the EC permeability coefficient of the tracer (P_{tracer}), the surface area of EC (S, cm^2), and the concentration gradient of the tracer between the plasma (C_{plasma}) and the interstitial fluid (C_{IF}): According to Fick's Law of diffusion, we obtain the equation: $J_{tracer} = P_{tracer} S (C_{plasma} - C_{IF})$[104]. Experimentally, the dosage of tracer administered, the time allowed between tracer injection and organ harvest, and the thoroughness of tissue washing are critical factors for the accuracy of this assay[2]. The severity of MVHP can be quantitatively analyzed by measuring histological images of the size and the degree of Evans blue staining, and/or by chromatography of Evans blue extracted from tissues, as illustrated in Figures 2, 4A and B[2,58,85]. A similar method has also been used in other organs with IRI, such as lungs[67,84] and the brain[105]. Evans blue in the circulation does not alter EC permeability per se. Whilst currently being used for animal studies only, it would be desirable to develop permeability tracers suitable for use in human patients, and that can be detected by imaging techniques.

Fluorescent-intensity imaging

This technique has been used for quantifying MVHP in pulmonary or brain injury models[67,99]. Clavijo *et al.* modified this technique for *in vivo* use to detect pulmonary MVHP using videomicroscopy through a surgical window over the chest and fluorescence tracer injection[67]. A lung window device is inserted through the chest incision and secured in place with sutures. Lungs are in contact with the window and visible through the glass coverslip. FITC-albumin is administered intravenously, and the experiment is performed in a dark room to observe the surface of pulmonary lobes. The imaging system includes a reflected-light microscope with epi-illumination (450-490 nm wavelength) and an objective lens (working distance 15 mm) connected to a high-resolution video camera to view and record fluorescence images[67].

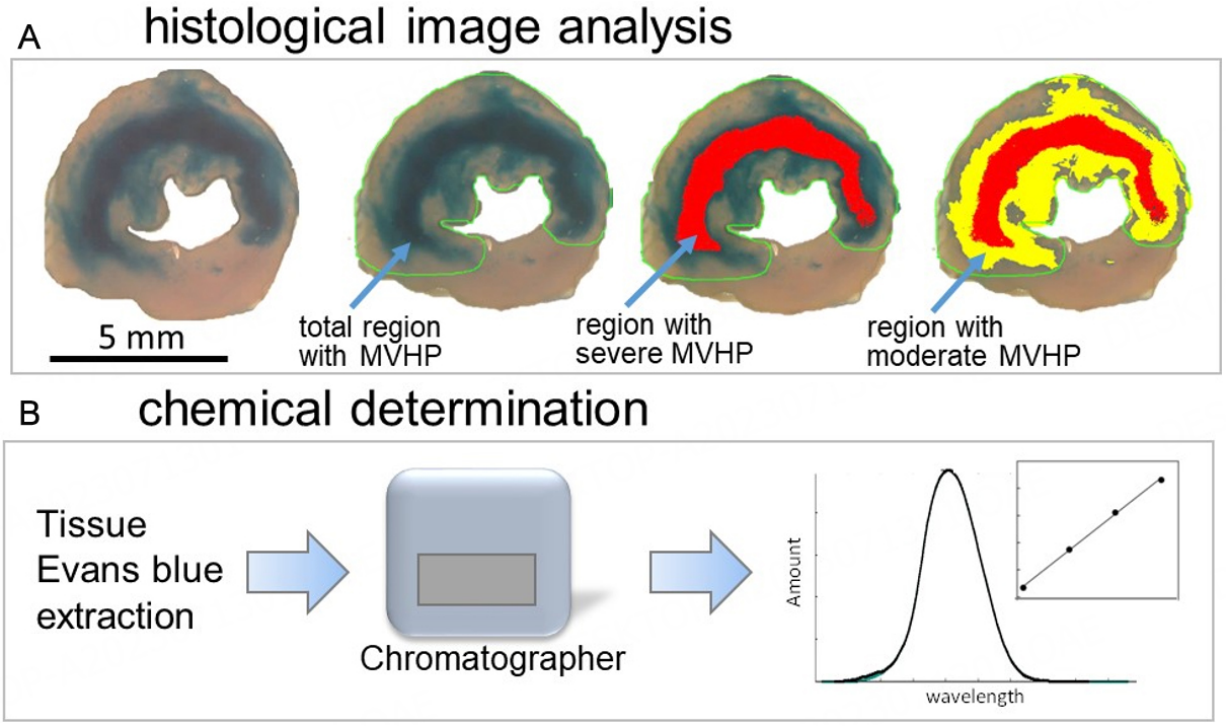

Figure 4. Determination of cardiac MVHP using Evans blue (EB) as a permeability tracer in mice subjected to IR (1/24 h). (A) Myocardial zones stained with EB indicating MVHP. The size and severity of MVHP in the mouse heart can be assessed histologically by contour analysis of serial sections for severe (red) or moderate (yellow) MVHP. (B) The severity of MVHP can also be estimated by biochemical assay of tissue EB content using chromatography. Adapted with permission from Ref.[2], Copyright © 2017 by American Physiological Society.

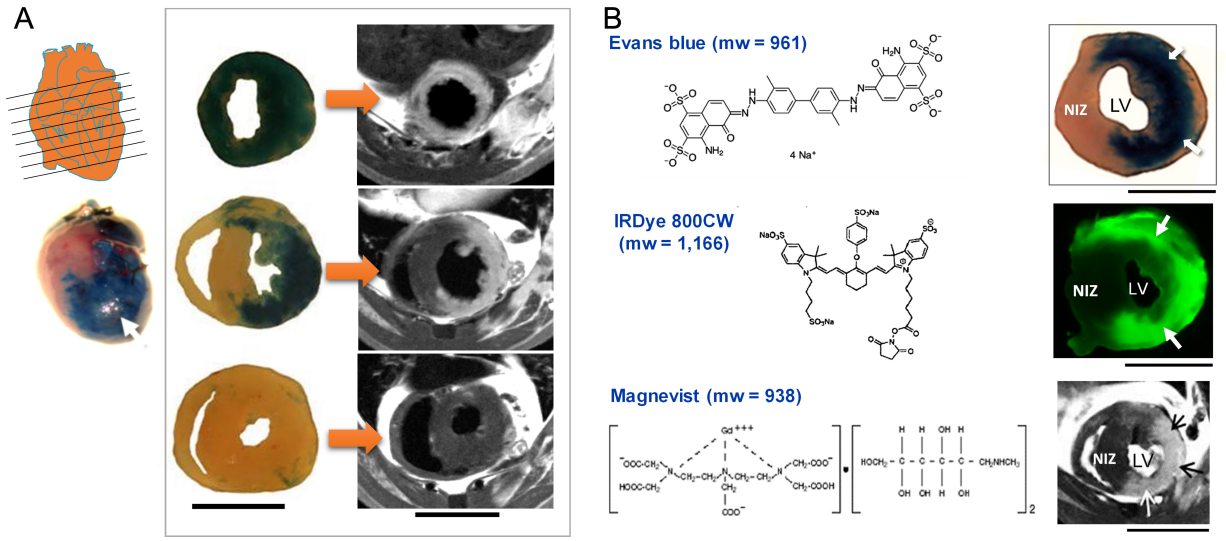

Figure 5. Validation of cardiac MRI-LGE-based detection of MVHP in mouse hearts with IRI. (A) The mice with IR were injected with Gd-contrast Megnevist (Bayer, 0.4 mmol/kg, i.v. 30 min before euthanasia), and cardiac MRI-LGE images were generated using a 9.4T Agilent scanner. After MRI, the mouse heart was transversely sectioned from the apex to the base with 0.8 mm thickness, equivalent to that of CMR imaging. (B) Mice were subjected to IR (1/24 h). Evans blue (20 mg/kg) and/or IRDye 800CW (50 l stock solution per mouse diluted in PBS) was administered i.v. 3 h before harvesting the heart. The heart was thoroughly flushed via an aortic cannula, and then cut transversely into 7-9 sections (approximately 0.8 mm thickness). IRDye fluorescent images of the sections were acquired (excitation 774 nm, emission 789 nm). The images show histological Sections from the apex to the base of the heart, with blue staining indicating MVHP and MRI-LGE. Orange arrows indicate histological and MRI-LGE images acquired at comparable levels of the heart. Bar = 5 mm. Adapted with permission from Ref.[2], Copyright © 2017 by American Physiological Society.

This method is potentially applicable for acute experimentation in the heart *in vivo*. Its drawbacks are the need for extensive surgery and a specialized imaging device. For *ex vivo* experiments using monolayer EC to determine EC permeability, either 2D (Transwell device) or 3D cell culture models have been described with the use of fluorescently labeled dextrans (40-150 kDa) as permeability tracers[85,104,106]. In addition, intravital microscopy together with fluorescent dye allows for direct visualization of MVHP in various organs[62,67].

Organ imaging techniques

By using different sequences or contrast (e.g., gadolinium Megnevist) [Figure 5B], MRI is the technique commonly used in animal or human studies to examine organ IRI and detect tissues with poor perfusion as a sign of lower early gadolinium enhancement (T1-EGE), myocardial infarction by T1-late gadolinium enhancement (T1-LGE), tissue edema, or tissue hemorrhage by T2* sequencing[22,23,27]. Imaging techniques of CT and MRI are commonly used for direct visualization of brain edema after ischemic stroke, together with midline shift and displacement of cerebrospinal fluid (CSF volumetrics) from the cerebral hemispheres, providing additional quantitative assessment of the severity[18,107-109].

Cardiac MRI permits a comprehensive evaluation of the infarcted heart. The mass of the myocardium with MRI-LGE has long been regarded as the gold standard marker for the infarct size. Interestingly, several studies have reported that the mass of cardiac MRI-LGE measured at the early phase post-IR (i.e., 1-2 days) is significantly larger than that determined from 3-7 days onwards[110-112]. And the reason for the overestimated infarct size is undefined. Using a mouse cardiac IRI model, we demonstrated that MVHP in the jeopardized myocardium can be visualized not only by Evans blue or fluorescence tracer [Figures 4, 5A and B][2,85], but also by cardiac MRI-LGE. This is evidenced by an excellent matching of the contour analyses of the size of the Evans blue-stained region by histology and that by cardiac MRI-LGE [Figure 5A][2]. This finding in the mouse heart provides an explanation for the overestimation of the infarct size by MRI-LGE in patients in the early phase post-IR, when the MVHP reaches its maximum[2,16,23].

Photoacoustic imaging is the technique-in-development that combines the high contrast of optical imaging with the spatial resolution of ultrasound imaging. Xu *et al.* used photoacoustic topography to image serial changes in brain edema induced by cold injury[113]. In a preliminary test using a mouse cardiac IRI model and a Visulsonic 2100/LAZR system, we acquired heart images [Figure 6A-C] showing that Evans blue, as a tissue MVHP tracer, is able to absorb energy from the laser beam, converting energy to heat and causing rapid tissue expansion that generates ultrasound waves. This finding, although made in an *ex vivo* heart, proves the concept for the feasibility of using MV permeability tracers with photoacoustic features for *in vivo* imaging of organ MVHP. Recently, Ding *et al.* described a brain imaging technique for cerebral tissue ischemia and edema by using optical coherence tomography combined with a photoacoustic microscope to achieve high spatial resolution (micron scale) vascular imaging as well as tissue properties. Using the rat model of acute ischemic stroke and free of contrast, they serially monitored changes in blood flow, vessel diameter, and the extent of edema for up to 5 h, with the latter being detectable as early as 30 min after ischemia[114]. These findings provide good examples for bilateral translation of preclinical-clinical research aiming at developing imaging techniques for MVHP detection.

Clinical imaging detection of MVHP

Several clinical indices have been routinely used for assessing the success of restoration of myocardial reperfusion by thrombolytic therapy or by primary percutaneous coronary intervention (PCI). These include catheter-based real-time angiography for myocardial tissue blush, recovery of elevated ST-T in electrocardiography post-PCI, the thrombolysis-in-myocardial-infarction score, or imaging-based techniques like contrast echocardiography, cardiac MRI with gadolinium contrast, or radionuclide angiography[15]. In contrast, MVHP has rarely been monitored as an indicator for the severity of cardiac IRI

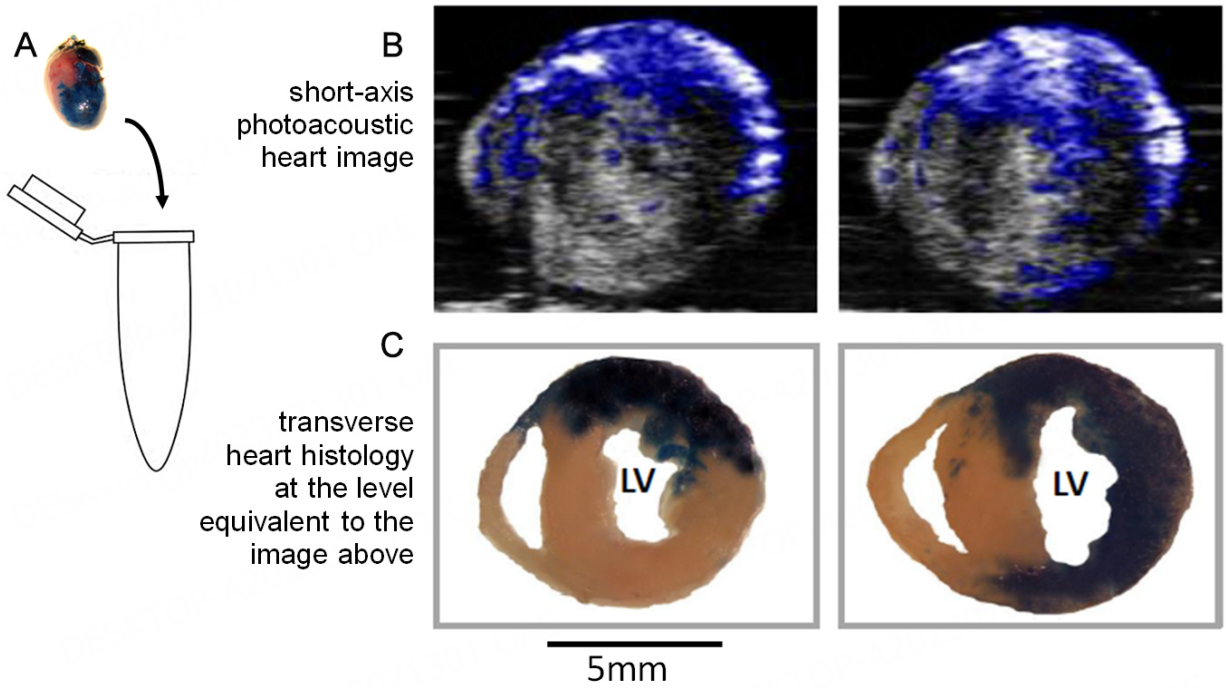

Figure 6. Photoacoustic imaging for detection of cardiac MVHP induced by IR. (A) Mice were subjected to IR (1/24 h), and Evans blue (EB) was administered 3 h prior to harvest of the heart. The flushed and isolated heart was positioned in an Eppendorf tube filled with ultrasound gel. (B) The photoacoustic imaging was acquired using the Visulsonic 2100/LAZR system, showing navy blue-white colors. Owing to the photoacoustic effect of EB accumulated within the jeopardized myocardium, the energy from the laser is absorbed by EB-containing tissues and then converted into ultrasonic waves due to transient thermoelastic expansion of the tissue. (C) The heart was then serially sectioned, and images with EB staining were compared with those of photoacoustic images. This set of images is from the author's unpublished study.

or for the efficacy of therapies. This situation, however, has been improving in the era of cardiac MRI. While in the last 25 years, cardiac MRI has been regarded as a golden method for determination of the infarct size[115], it is only in the last decade that the significance of MRI signs of tissue edema and IMH has been increasingly appreciated[21,22,25-27,29,30]. Clinical imaging studies on patients with reperfused MI have revealed equal or even higher percentages of MRI-detected myocardial edema (30%-70%) and IMH (35%-50%) relative to that of the "no-reflow" phenomenon (25%-50%)[17,24,25,27,30,116-118]. In the setting of ischemic stroke, CT imaging is able to detect extravasation of contrast agent (e.g., iodine) as well as intracranial hemorrhage[119]. Imaging-based detection of BBB disruption by contrast extravasation has long been used in the clinic[100,105,108,120]. In patients with ischemic stroke who underwent thrombectomy, CT imaging conducted 24 h afterward detected moderate BBB disruption in nearly 30% of cases, and this sign was associated with a high risk of hemorrhagic transformation and hematoma[121]. Another MRI study on ischemic stroke patients revealed that the region with BBB disruption is highly likely to become infarcted[122].

MVHP-related blood biomarkers

Development of the panel of MVD-related biomarkers is still in an early and translational stage[26,46,123,124]. Some biomarkers are proposed to reflect EC damage, such as molecules from glycocalyx shedding (syndecan-1, hyaluronan, heparin sulfate) [Figure 3B], claudins (tight-junction proteins), inflammatory markers, and adhesion molecules. Currently, there are a limited number of clinical studies that have explored biomarkers for MVHP validated by using other clinical signs of MVHP in cardiac IRI. In patients with ischemic stroke, however, accumulating studies have demonstrated elevation of a panel of biomarkers, together with clinical imaging examination, for the loss of BBB integrity. These studies found that around 24-48 h after admission, there were elevated serum levels of markers including MMP-2, MMP-9,

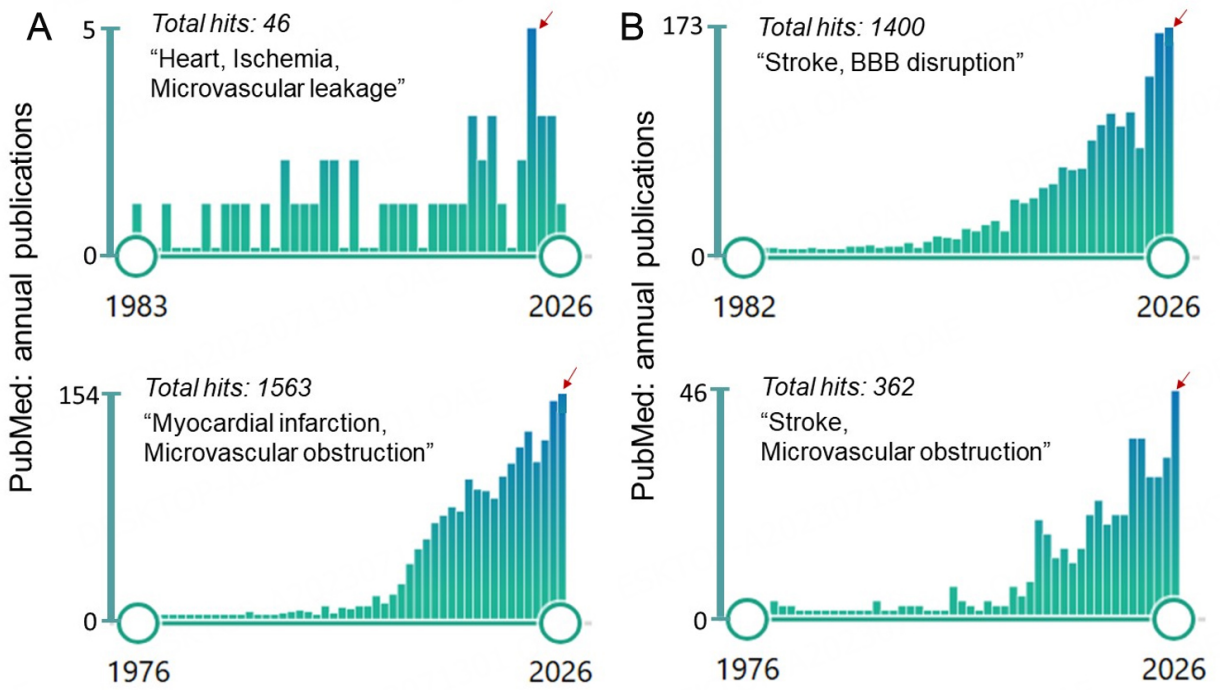

Figure 7. Number of publications per year on MVO or MVHP (or MV leakage) in settings of cardiac ischemia/infarction (A) or stroke (B). The graph is generated from a PubMed search using combinations of keywords as indicated in each panel. Note that the total number of publications on MVHP is far less for cardiac ischemia/infarction relative to that in stroke, reflecting the presence of preconception on the MVD pathophysiology in cardiac IRI. The scale of the Y-axis is based on the highest annual number of publications per panel indicated with a red arrow.

neuron-specific enolase, S100B, occludin, inflammatory markers, glycocalyx degradation and shedding (hyaluronan, syndecan), hypoxanthine and metabolites (methionine, acetate), and that their elevation was associated with imaging-detectable contrast extravasation (brain edema) and more severe brain injury[26,46,119,123].

THERAPEUTIC INTERVENTIONS TARGETING MVHP

Clinical studies on MVHP-targeted therapies

Significance of the "no-reflow" phenomenon following acute MI has long been fully recognized, and post-MI reperfusion therapy by medicine and/or catheter devices is the current clinical routine for functional preservation and limiting the infarct size and left ventricular (LV) remodeling[5,7,10,12]. Numerous clinical studies have tested MVD-targeted therapies, such as intracoronary or intracerebral vasodilators (adenosine, nitroprusside, Ca^{2+}-channel blockers, -blockers), anti-inflammatory agents, remote ischemic preconditioning, or supersaturated oxygen delivery (for review[10,13-15]). While these studies showed certain benefits estimated by improved tissue perfusion flow or angiography-derived index of microcirculatory resistance, the indices reflecting cardiac MVHP have rarely been determined in these clinical studies. This situation is in contrast to the field of ischemic stroke, where BBB disruption is well recognized in causing tissue damage and subsequent neurological deficits and long-term functional impairments [Figure 7][63,64,114,119,121,122,125]. Clinical appreciation of the significance of BBB disruption promotes active research on post-stroke BBB disruption and restoration. Recent clinical studies reported that normobaric hyperoxygenation is effective in preserving BBB integrity, judged by serum BBB markers (MMP-9, enolase, S100B, occludin) as well as imaging findings[119]. Through tedious biochemical screening in patients or mice with ischemic stroke, Ye *et al.* identified higher serum levels of hypoxanthine as a new marker of BBB disruption in stroke, and that hypoxanthine participates in EC pyroptosis, forming a new therapeutic target[123].

Summary of preclinical *in vivo* findings

Over the last several decades, preclinical studies have intensively investigated therapies against IRI. However, the majority of studies only measured the acute-phase change in infarct size to evaluate therapeutic efficacy, and the potential influence of interventions on MVHP has not been examined. With the recent appreciation of the significance of MVHP and the unmet clinical need for medications, there has been an increasing number of preclinical studies on *in vivo* models of IRI in the heart and brain with findings showing amelioration of MVHP by pharmacological interventions [Table 1]. In all studies included in Table 1, cardiac or brain MV barrier function was ascertained by histology and/or imaging detection of tissue edema and MV permeability analyses. Several studies on cardiac IRI have provided evidence for inhibition of MVHP together with reduced extent of LV remodeling at a chronic phase[85,90,126]. In some studies, effects of specific agonists or inhibitors were confirmed by EC-restricted gene deletion or siRNA gene targeting of desired proteins[58,68,76,91,127]. Some drugs were found not only to reduce cardiac MVHP, but also to reduce the size of MVO (no-reflow) or infarct[15,85,126,128].

In cultured ECs or *in vivo* IRI models, prevention of intracellular Ca^{2+} overload using blockers of Ca^{2+} channels or TRPV4 channels has been shown to ameliorate MVHP[57,58,105]. In a cerebral ischemic model, treatment with the mitochondrial protective agent bendavia limited IRI-induced Ca^{2+} accumulation in ECs or pericytes, oxidative stress, mitochondrial dysfunction, and MVHP[129]. Relevant to Ca^{2+} overload in ECs is a rapid activation of aquaporin 4 water channels by enhanced Ca^{2+} entry, in part through TRPV4 channels. In the ischemic stroke model, inhibition of aquaporin 4 using methylene blue reduced the severity of brain edema[105,130,131]. A few drugs tested recently in brain IRI models exhibited protection against BBB disruption by directly stabilizing EC junctions (e.g., EphA4 inhibitor or Y-27632)[132,133]. Losartan is a well-known angiotensin II type-1 receptor (AT1R) antagonist with cardiovascular protective properties. Li *et al.* found in a murine cardiac IRI model that treatment with losartan preserved MV permeability, reduced myocardial edema and inflammation, and limited the infarct size[126]. The EC protective mechanism of losartan involves inhibition of Src activation and preservation of VE-cadherin expression[126]. Chappell *et al.* showed that treatment with antithrombin or hydrocortisone is effective in the preservation of endothelial glycocalyx and MV permeability in animal models of cardiac or brain IRI[42,89]. Drugs that promote protective mitophagy, such as empagliflozin, were effective in limiting MVHP in the mouse model of cardiac IRI[134]. Studies have also confirmed the protective efficacy of test chemicals with the use of genetic inhibition of target molecules[62,68,97,135]. Several transcription factors or cofactors are found to be involved in MVHP. Transcription factor nuclear receptor subfamily 4 group A member 1 (Nr4a1) is mainly expressed in vascular cells and is rapidly activated or upregulated upon IRI, and Nr4a1 gene-deleted mice showed reduced MVHP following pulmonary transplantation[136]. mitoQ was reported to limit MVHP in lungs or intestines subjected to IRI by activating nuclear factor erythroid 2-related factor 2, which is known to induce expression of anti-oxidative genes[137]. In the brain IRI model, expression of a transcription co-regulator, yes-associated protein (YAP), was upregulated, and inhibition of nuclear YAP activity using verteporfin reduced MVHP[76]. This finding is interesting given that YAP is well-known as a mechanotransduction-sensing molecule in cardiovascular cells, including ECs[138,139], and that under physiological and pathological conditions YAP regulates cellular responses to mechanical stimuli with increased intracellular Ca^{2+}[139]. Certain Chinese medicines have been reported to effectively minimize MVHP under conditions of organ IRI, with the mechanisms in part due to the maintenance of mitochondrial function and reduction in ROS[50,93,140,141].

Some drugs were found to possess potent anti-inflammatory properties [Table 1]. In a model of pulmonary MVHP induced by platelet lysate or G-endotoxemia, treatment with WEB-2086, an inhibitor of PAF receptor, limited MVHP[33,67]. Protection against MVHP was also observed in brain or cardiac IRI models by using an anti-VEGF antibody[142]. Treatment with an Epac agonist terminated MVHP through promoting eNOS translocation from cytosol to cell membrane[33]. Several drugs like CU06-1004[65,128] and relaxin[85] or

gene deletion of USP30 (a mitochondrial deubiquitination enzyme)[84] are potent in inhibiting MVHP together with a strong anti-inflammatory effect [Table 1]. In the cardiac IRI model, relaxin treatment significantly reduced the severity of MVHP, together with preservation of VE-cadherin and reduction in the area of MVO[85], efficacy that led to limited LV remodeling measured by LV end-diastolic volume at 2 weeks post-IRI, although the infarct size was not changed by relaxin treatment[85]. In ECs cultured in monolayer using a Transwell culture device, treatment with relaxin also reversed MVHP induced by hypoxia-reoxygenation, ROS (H_2O_2), or cytokines (IL-1 or macrophage-migration inhibitory factor)[85]. Sac-1004 is a pseudo-sugar derivative of cholesterol and was found in the rat model of ischemic stroke to limit MVHP[143]. As shown in Table 1, several recent studies on stroke models revealed that test drugs (e.g., Sac-1004, combination of JNJ0966 and BI-0115, A@HPB@THSA, SYS18, or miR-383-5p) limited BBB disruption together with strong anti-inflammatory and/or anti-ROS actions[140,143-146].

Limitations of preclinical studies on MVHP-targeted therapy

Owing to the relatively limited number of publications on MVHP in the heart and brain post-IRI, it is premature to draw conclusions on similarities or organ specificity in MVHP-targeted therapies, albeit certain classes of drugs appear to be effective in both settings [Table 1]. Also shown in Table 1, in many studies, test drugs were delivered at the time of reperfusion, which is clinically achievable. However, it is hard to address the issue of reproducibility of findings made in individual laboratories given the specific experimental models and protocols of therapeutic regimens. The therapeutic window across the spectrum from MVHP to MV disruption remains unclear. In fact, there has been no report that has taken the onset and severity of IMH, an index of MV disruption, as endpoints in evaluating therapeutic efficacy. One obvious reason for this is that, unlike MVHP as a regulated and reversible process, IMH represents irreversible MV damage [Figure 3C]. However, it is important to appreciate the dynamic evolution of MVHP, as depicted in Figure 3, and the fact that within the ischemic region, the severity of MVHP/MV disruption is highly heterogeneous [Figures 2 and 4]. Hence, it is likely that therapeutic efficacy is achievable by MVHP-targeted therapy delivered in the early phase of IRI.

CONCLUDING REMARKS

MVHP represents a pivotal pathophysiological and clinical entity in organ IRI

A full appreciation of the spectrum of MVD, particularly MVHP, has reshaped our understanding of IRI pathophysiology, in which microvascular ECs constitute a cell type vulnerable to IRI and important in determining organ injury. As discussed in this review, preclinical and clinical studies conducted in the last two decades have documented MVHP/MV disruption as a common event contributing to tissue edema, inflammatory infiltration, MVO, and IMH. Being an early event of IRI, MVHP constitutes a pivotal mechanism impacting the overall outcome of organ IRI. Several techniques for the determination of MVHP are discussed in this review. Accordingly, it is timely and important to establish the techniques and parameters of MVHP monitoring applicable in routine clinical practice as well as in laboratory research. Similarly, the therapeutic strategy of IRI needs to be updated by focusing not only on the jeopardized myocardium, i.e., limiting the infarct size, but also on protection and restoration of MV function and integrity. Further research is urgently needed to identify therapeutic targets and establish effective interventions for limiting MVHP.

Overcoming translation barriers

In this research field, translational barriers exist on both clinical and preclinical aspects. Insufficient appreciation of the spectrum of MVD in general and the significance of MVHP in particular may represent a key knowledge gap, which could impact the planning of clinical and preclinical research. As discussed in this review, MVO and MVHP might differ significantly in the pathogenesis and hence the therapeutic interventions. Furthermore, while biomarkers are a significant part of clinical practice in modern cardiology,

particularly in acute MI, their clinical use for MVO and MVHP remains immature.

While the significance of MVHP in myocardial infarction begins to draw attention, correction of our preconception on MVD is apparently far behind the area of stroke as a cross-discipline example, as implicated by the sharp difference in the number of publications on MVHP/leakage in cardiac versus brain IRI [Figure 7]. BBB disruption has long been emphasized as a pivotal index with diagnostic, therapeutic, and prognostic significance[64,100,119,125,130]. And based on research findings on the pathophysiology of BBB disruption in stroke[63,64,147], therapies have either been established or proposed in clinical research targeting glycocalyx preservation, stabilizing pericytes[148,149] and overcoming EC mitochondrial dysfunction[129,150].

Clinical research is encouraged to test adjunctive therapies for IRI with MVHP or IMH as endpoints. One obvious advantage of such clinical trials is that, owing to catheter-based interventions in patients with acute MI or stroke, it is feasible to administer test drugs via intra-arterial catheter to achieve timely drug delivery at desired dosages while reducing the potential side effects due in part to the systemic route. Indeed, there are preclinical studies showing that a single dose of test drugs delivered prior to or after reperfusion yielded significant efficacy[85,128].

Preclinically, there exist significant translational barriers as well. In therapeutic studies, animals are usually young and healthy immediately prior to IRI, and almost all studies were done using rodents (mice, rats), single laboratory-based, insufficient validation either studying in large laboratory species or by cardiac imaging or blood biomarkers of human patients. One aspect for improvement is to test drugs in aged animals or in animals with comorbidities to better simulate clinical entities. Current experimental studies testing new drugs might also be limited in short-term assessment of drug efficacy without exploring the long-term outcomes. Here, the option for better research translation is to integrate clinically relevant models, MVHP-specific endpoints, mechanical interventions, and pharmacological adjuncts instead of using them in isolation. In this field, imaging techniques and the use of blood biomarkers should become important tools in facilitating research translation.

Future key research questions

The roadmap for research translation of MVHP might include a number of important questions. First, for preclinical and clinical research on MVHP, it is essential to establish quantitative techniques and standardized diagnostic criteria for MVHP. As discussed in this review, parameters could be based on histology, permeability indicators, contrast imaging, and biomarkers. With the development of facilities for bedside cardiac MRI, clinical investigation of MVD/MVHP/IMH would certainly be encouraged. Efforts should be made to develop tracers for image-based direct viewing of MVHP of jeopardized organs. Simultaneous determination of MVHP and phenotypic parameters of MVD, including tissue hemorrhage, MVO, and infarct size, would be valuable for evaluating the specific impact of MVHP on the overall spectrum of MVD and organ damage. Second, biomarker research should be routine in laboratory studies of MVD and MVHP. *In vivo* animal models offer clear advantages: precise IR timing, controlled IRI severity, self-validation through simultaneous assays of biomarkers in blood and heart tissue, and an established platform for EC-restricted gene modification. Given that microvascular ECs account for approximately 50% of the cardiac cell population and their localization at the tissue-circulation interface, a rich body of EC-derived biomarkers is expected to exist in the setting of IRI. Here, Imaging findings of MVHP, if complemented by assays of blood biomarkers, would be invaluable for translational purposes. Third, clinical trials testing interventions on MVHP should be encouraged. When conducted in catheter laboratories, clinical interventions for MVHP and MVO would benefit from timely, precise drug delivery through reopened culprit arteries. Notably, an early and short-term treatment is likely to be effective based on current preclinical findings. As addressed in this review, the severity of MVHP can be highly heterogeneous across

the ischemic region[2], and the image-identified prevalence of IMH increases within 7 days post-MI[21]. Thus, there may be a relatively wide therapeutic time window, when therapy is expected to be beneficial even in the continued presence of pathological stimuli derived from damaged myocardium or infiltrated inflammatory cells. Given our understanding of MVHP pathophysiology and the multiple factors driving its development [Figure 3], the combined therapeutic regimen is expected to be more effective at halting the deterioration of MVHP into the irreversible phase characterized by EC/pericyte death and MV structural disruption. In addition to anti-inflammatory drugs[33], certain interventions would be worthwhile to test, aiming at preservation of EC mitochondrial function, e.g., mitochondrial delivery, nanomedicines targeting ROS or cell death signaling, and activators of endogenously protective signaling in EC such as S1PR1, Epac, or eNOS [Table 1]. Finally, it remains undefined which factors not only induce but also sustain MVHP, driving towards irreversible MV disruption. The severity of MVD/MVHP is heterogeneous across the jeopardized region. Similar to the concept of limiting the infarct size, prevention of phased transition from reversible MVHP to MV disruption should be taken as one of the primary therapeutic targets. Here, interactions between microvascular EC and blood cells are critical in the progression of MVHP and therefore deserve to be considered for therapeutic intervention.

DECLARATIONS

Author contribution

The author contributed solely to the article.

Availability of data and materials

The data presented in this study are available on request from the corresponding author.

AI and AI-assisted tools statement

The visual elements illustrating MVHP and MVO in the graphical abstract and Figure 1 were created with PicDoc (https://www.picdoc.cn, beta version), an AI-powered text-to-visualization tool. The AI tool did not influence the study design, data collection, analysis, interpretation, or the scientific content of the work. The author takes full responsibility for the accuracy, integrity, and final content of the manuscript.

Financial support and sponsorship

None.

Conflict of interest

Du XJ is an Editorial Board Member of the journal *Vessel Plus* and a Guest Editor of the Special Issue "Microvascular Damage". Du XJ was not involved in any aspect of the editorial processing of this manuscript, including reviewer selection, manuscript handling, and decision-making.

Ethical approval and consent to participate

Not applicable.

Consent for publication

Not applicable.

Copyright

© The Author(s) 2026.

REFERENCES

1. Du XJ. Post-infarct cardiac injury, protection and repair: roles of non-cardiomyocyte multicellular and acellular components. *Sci China Life Sci.* 2018;61:266-76. DOI PubMed

2. Gao XM, Wu QZ, Kiriazis H, et al. Microvascular leakage in acute myocardial infarction: characterization by histology, biochemistry, and magnetic resonance imaging. *Am J Physiol Heart Circ Physiol.* 2017;312:H1068-75. DOI PubMed
3. Ito H. No-reflow phenomenon and prognosis in patients with acute myocardial infarction. *Nat Clin Pract Cardiovasc Med.* 2006;3:499-506. DOI PubMed
4. Kloka JA, Friedrichson B, Wülfroth P, Henning R, Zacharowski K. Microvascular leakage as therapeutic target for ischemia and reperfusion injury. *Cells.* 2023;12:1345. DOI PubMed PMC
5. Kloner RA. No-reflow phenomenon: maintaining vascular integrity. *J Cardiovasc Pharmacol Ther.* 2011;16:244-50. DOI PubMed
6. Bulluck H, Hausenloy DJ. Reperfusion injury and infarct size: why translation has been difficult, and how we move forward. *Curr Cardiol Rep.* 2026;28:78. DOI PubMed PMC
7. Heusch G, Gersh BJ. The pathophysiology of acute myocardial infarction and strategies of protection beyond reperfusion: a continual challenge. *Eur Heart J.* 2017;38:774-84. DOI PubMed
8. Kloner RA. Current state of clinical translation of cardioprotective agents for acute myocardial infarction. *Circ Res.* 2013;113:451-63. DOI PubMed
9. Takemura G, Nakagawa M, Kanamori H, Minatoguchi S, Fujiwara H. Benefits of reperfusion beyond infarct size limitation. *Cardiovasc Res.* 2009;83:269-76. DOI PubMed
10. Cenko E, Badimon L, Vadalà G, et al. Pathophysiology, prevention, and management of coronary microvascular obstruction. *Eur Heart J.* 2026;47:4215-41. DOI PubMed
11. Gadelmawla AF, Taha AM, Alkuwaiti FA, et al. Prognostic impact of persistent microvascular obstruction on cardiac magnetic resonance after STEMI: a systematic review and meta-analysis. *Int J Cardiol.* 2026;456:134523. DOI PubMed
12. Galli M, Niccoli G, De Maria G, et al. Coronary microvascular obstruction and dysfunction in patients with acute myocardial infarction. *Nat Rev Cardiol.* 2024;21:283-98. DOI PubMed
13. Maino A, Walsh JL, Portolan L, et al. Therapeutic interventions for coronary microvascular obstruction after acute myocardial infarction: developments and challenges. *Pharmacol Ther.* 2026;282:108995. DOI PubMed
14. Ndrepepa G, Kastrati A. Coronary no-reflow after primary percutaneous coronary intervention-current knowledge on pathophysiology, diagnosis, clinical impact and therapy. *J Clin Med.* 2023;12:5592. DOI PubMed PMC
15. Rezkalla SH, Stankowski RV, Hanna J, Kloner RA. Management of no-reflow phenomenon in the catheterization laboratory. *JACC Cardiovasc Interv.* 2017;10:215-23. DOI PubMed
16. Bonfig NL, Soukup CR, Shah AA, et al. Increasing myocardial edema is associated with greater microvascular obstruction in ST-segment elevation myocardial infarction. *Am J Physiol Heart Circ Physiol.* 2022;323:H818-24. DOI PubMed
17. Fernández-Jiménez R, Sánchez-González J, Agüero J, et al. Myocardial edema after ischemia/reperfusion is not stable and follows a bimodal pattern: imaging and histological tissue characterization. *J Am Coll Cardiol.* 2015;65:315-23. DOI PubMed
18. Wan Y, Holste KG, Hua Y, Keep RF, Xi G. Brain edema formation and therapy after intracerebral hemorrhage. *Neurobiol Dis.* 2023;176:105948. DOI PubMed PMC
19. Xi G, Hua Y, Bhasin RR, Ennis SR, Keep RF, Hoff JT. Mechanisms of edema formation after intracerebral hemorrhage: effects of extravasated red blood cells on blood flow and blood-brain barrier integrity. *Stroke.* 2001;32:2932-8. DOI PubMed
20. Frangogiannis NG. Pathophysiology of myocardial infarction. *Compr Physiol.* 2015;5:1841-75. DOI PubMed
21. Amier RP, Tijssen RYG, Teunissen PFA, et al. Predictors of intramyocardial hemorrhage after reperfused ST-segment elevation myocardial infarction. *J Am Heart Assoc.* 2017;6:e005651. DOI PubMed PMC
22. Berry C, Carberry J, Dharmakumar R. Intramyocardial hemorrhage after myocardial infarction: a prognostic outcome for clinical practice and trials. *Circulation.* 2025;152:349-51. DOI PubMed
23. Carrick D, Haig C, Ahmed N, et al. Temporal evolution of myocardial hemorrhage and edema in patients after acute ST-segment elevation myocardial infarction: pathophysiological insights and clinical implications. *J Am Heart Assoc.* 2016;5:e002834. DOI PubMed PMC
24. Eitel I, Kubusch K, Strohm O, et al. Prognostic value and determinants of a hypointense infarct core in T2-weighted cardiac magnetic resonance in acute reperfused ST-elevation-myocardial infarction. *Circ Cardiovasc Imaging.* 2011;4:354-62. DOI PubMed
25. Hamirani YS, Wong A, Kramer CM, Salerno M. Effect of microvascular obstruction and intramyocardial hemorrhage by CMR on LV remodeling and outcomes after myocardial infarction: a systematic review and meta-analysis. *JACC Cardiovasc Imaging.* 2014;7:940-52. DOI PubMed PMC
26. Tiller C, Reindl M, Holzknecht M, et al. Association of intramyocardial hemorrhage with inflammatory biomarkers in patients with ST-segment elevation myocardial infarction. *JACC Adv.* 2025;4:101647. DOI PubMed PMC
27. Vora KP, Kumar A, Krishnam MS, Prato FS, Raman SV, Dharmakumar R. Microvascular obstruction and intramyocardial hemorrhage in reperfused myocardial infarctions: pathophysiology and clinical insights from imaging. *JACC Cardiovasc Imaging.* 2024;17:795-810. DOI PubMed PMC

28. Chan W, White DA, Wang XY, et al. Macrophage migration inhibitory factor for the early prediction of infarct size. *J Am Heart Assoc.* 2013;2:e000226. DOI PubMed PMC
29. Huang Y, Guan X, Zhang X, et al. Accurate intramyocardial hemorrhage assessment with fast, free-running, cardiac quantitative susceptibility mapping. *Radiol Cardiothorac Imaging.* 2024;6:e230376. DOI PubMed PMC
30. Tyler A, Li Kam Wa ME, Littlewood SJ, et al. An initial clinical evaluation of quantitative susceptibility mapping for quantitative characterisation of intramyocardial hemorrhage. *J Cardiovasc Magn Reson.* 2026;28:102707. DOI PubMed PMC
31. Gao XM, Xu Q, Kiriazis H, Dart AM, Du XJ. Mouse model of post-infarct ventricular rupture: time course, strain- and gender-dependency, tensile strength, and histopathology. *Cardiovasc Res.* 2005;65:469-77. DOI PubMed
32. Liu Y, Gao XM, Fang L, et al. Novel role of platelets in mediating inflammatory responses and ventricular rupture or remodeling following myocardial infarction. *Arterioscler Thromb Vasc Biol.* 2011;31:834-41. DOI PubMed
33. Nepali PR, Burboa PC, Lillo MA, et al. Endothelial mechanisms for inactivation of inflammation-induced hyperpermeability. *Am J Physiol Heart Circ Physiol.* 2023;324:H610-23. DOI PubMed PMC
34. Gawaz M, Langer H, May AE. Platelets in inflammation and atherogenesis. *J Clin Invest.* 2005;115:3378-84. DOI PubMed PMC
35. Abassi Z, Armaly Z, Heyman SN. Glycocalyx degradation in ischemia-reperfusion injury. *Am J Pathol.* 2020;190:752-67. DOI PubMed
36. Butler MJ, Down CJ, Foster RR, Satchell SC. The pathological relevance of increased endothelial glycocalyx permeability. *Am J Pathol.* 2020;190:742-51. DOI PubMed PMC
37. Chappell D, Jacob M, Paul O, et al. The glycocalyx of the human umbilical vein endothelial cell: an impressive structure ex vivo but not in culture. *Circ Res.* 2009;104:1313-7. DOI PubMed
38. Dogné S, Flamion B. Endothelial glycocalyx impairment in disease: focus on hyaluronan shedding. *Am J Pathol.* 2020;190:768-80. DOI PubMed
39. Miranda CH. Longitudinal assessment of endothelial glycocalyx in ST-elevation myocardial infarction: interplay with oxidative stress and inflammation. *Microvasc Res.* 2026;165:104926. DOI PubMed
40. Bayam E, Kalçık M, Gürbüz AS, Özkan M. The emerging role of heparanase in cardiovascular diseases: pathophysiology, clinical outcomes, and therapeutic perspectives. *J Thromb Thrombolysis.* 2026;59:1142-57. DOI PubMed PMC
41. Chappell D, Hofmann-Kiefer K, Jacob M, et al. TNF-alpha induced shedding of the endothelial glycocalyx is prevented by hydrocortisone and antithrombin. *Basic Res Cardiol.* 2009;104:78-89. DOI PubMed
42. Chappell D, Jacob M, Hofmann-Kiefer K, et al. Antithrombin reduces shedding of the endothelial glycocalyx following ischaemia/reperfusion. *Cardiovasc Res.* 2009;83:388-96. DOI PubMed
43. van Golen RF, van Gulik TM, Heger M. Mechanistic overview of reactive species-induced degradation of the endothelial glycocalyx during hepatic ischemia/reperfusion injury. *Free Radic Biol Med.* 2012;52:1382-402. DOI PubMed
44. Vieira de Almeida MC, Zotin MCZ, Miranda CH. Systemic endothelial glycocalyx shedding mediates vascular hyperpermeability after traumatic brain injury. *Front Neurol.* 2025;16:1706102. DOI PubMed PMC
45. Zhu J, Li Z, Ji Z, et al. Glycocalyx is critical for blood-brain barrier integrity by suppressing caveolin1-dependent endothelial transcytosis following ischemic stroke. *Brain Pathol.* 2022;32:e13006. DOI PubMed PMC
46. Vignoli A, Sticchi E, Piccardi B, et al. Predicting reperfusion injury and functional status after stroke using blood biomarkers: the STROKELABED study. *J Transl Med.* 2025;23:491. DOI PubMed PMC
47. Bongoni AK, Lu B, McRae JL, et al. Complement-mediated damage to the glycocalyx plays a role in renal ischemia-reperfusion injury in mice. *Transplant Direct.* 2019;5:e341. DOI PubMed PMC
48. Salmon AHJ, Ferguson JK, Burford JL, et al. Loss of the endothelial glycocalyx links albuminuria and vascular dysfunction. *J Am Soc Nephrol.* 2012;23:1339-50. DOI PubMed PMC
49. Mondal NK, Behera J, Kelly KE, George AK, Tyagi PK, Tyagi N. Tetrahydrocurcumin epigenetically mitigates mitochondrial dysfunction in brain vasculature during ischemic stroke. *Neurochem Int.* 2019;122:120-38. DOI PubMed PMC
50. Wei X, Wu Y, Pan H, et al. Proteomics revealed that mitochondrial function contributed to the protective effect of Herba Siegesbeckiae against cardiac ischemia/reperfusion injury. *Front Cardiovasc Med.* 2022;9:895797. DOI PubMed PMC
51. Zhou H, Zhou H, Hu S, et al. Mff-dependent mitochondrial fission contributes to the pathogenesis of cardiac microvasculature ischemia/reperfusion injury via induction of mROS-mediated cardiolipin oxidation and HK2/VDAC1 disassociation-involved mPTP opening. *J Am Heart Assoc.* 2017;6:e005328. DOI PubMed PMC
52. Zhong J, Tan Y, Lu J, et al. Therapeutic contribution of melatonin to the treatment of septic cardiomyopathy: a novel mechanism linking Ripk3-modified mitochondrial performance and endoplasmic reticulum function. *Redox Biol.* 2019;26:101287. DOI PubMed PMC
53. Imai T, Iwata S, Hirayama T, et al. Intracellular Fe^{2+} accumulation in endothelial cells and pericytes induces blood-brain barrier dysfunction in secondary brain injury after brain hemorrhage. *Sci Rep.* 2019;9:6228. DOI PubMed PMC
54. Andjelkovic AV, Xiang J, Stamatovic SM, et al. Endothelial targets in stroke: translating animal models to human. *Arterioscler Thromb Vasc Biol.* 2019;39:2240-7. DOI PubMed PMC

55. Di Napoli P, Taccardi AA, Grilli A, et al. Verapamil reduces coronary endothelium damage and cardiomyocyte necrosis but not apoptosis after ischemia and reperfusion: ex-vivo study in rat hearts. *Int J Immunopathol Pharmacol.* 2002;15:225-32. DOI PubMed
56. Lan CC, Peng CK, Tang SE, et al. Inhibition of Na-K-Cl cotransporter isoform 1 reduces lung injury induced by ischemia-reperfusion. *J Thorac Cardiovasc Surg.* 2017;153:206-15. DOI PubMed
57. McDonagh PF, Roberts DJ. Prevention of transcoronary macromolecular leakage after ischemia-reperfusion by the calcium entry blocker nisoldipine. direct observations in isolated rat hearts. *Circ Res.* 1986;58:127-36. DOI PubMed
58. Zhang M, Zou Y, Ruan H, et al. Activation of endothelial TRPV4 exacerbates myocardial ischemia-reperfusion injury via vascular integrity impairment. *Can J Cardiol.* 2026;42:1353-65. DOI PubMed
59. Allen C, Srivastava K, Bayraktutan U. Small GTPase RhoA and its effector rho kinase mediate oxygen glucose deprivation-evoked in vitro cerebral barrier dysfunction. *Stroke.* 2010;41:2056-63. DOI PubMed
60. Anquetil T, Solinhac R, Jaffre A, et al. PI3KC2beta inactivation stabilizes VE-cadherin junctions and preserves vascular integrity. *EMBO Rep.* 2021;22:e51299. DOI PubMed PMC
61. Zheng T, Jiang T, Ma H, Zhu Y, Wang M. Targeting PI3K/Akt in cerebral ischemia reperfusion injury alleviation: from signaling networks to targeted therapy. *Mol Neurobiol.* 2024;61:7930-49. DOI PubMed
62. Shen Q, Rigor RR, Pivetti CD, Wu MH, Yuan SY. Myosin light chain kinase in microvascular endothelial barrier function. *Cardiovasc Res.* 2010;87:272-80. DOI PubMed PMC
63. Abdullahi W, Tripathi D, Ronaldson PT. Blood-brain barrier dysfunction in ischemic stroke: targeting tight junctions and transporters for vascular protection. *Am J Physiol Cell Physiol.* 2018;315:C343-56. DOI PubMed PMC
64. Gao HM, Chen H, Cui GY, Hu JX. Damage mechanism and therapy progress of the blood-brain barrier after ischemic stroke. *Cell Biosci.* 2023;13:196. DOI PubMed PMC
65. Noh M, Kim Y, Zhang H, et al. Oral administration of CU06-1004 attenuates vascular permeability and stabilizes neovascularization in retinal vascular diseases. *Eur J Pharmacol.* 2023;939:175427. DOI PubMed
66. Tsugawa-Shimizu Y, Fujishima Y, Kita S, et al. Increased vascular permeability and severe renal tubular damage after ischemia-reperfusion injury in mice lacking adiponectin or T-cadherin. *Am J Physiol Endocrinol Metab.* 2021;320:E179-90. DOI PubMed PMC
67. Clavijo LC, Carter MB, Matheson PJ, Wilson MA, Wead WB, Garrison RN. PAF increases vascular permeability without increasing pulmonary arterial pressure in the rat. *J Appl Physiol.* 2001;90:261-8. DOI PubMed
68. Zhao XY, Xu R, Li JJ, et al. S1PR1-MYPT1 maintains coronary endothelial barrier in pressure-overloaded hearts. *Hypertension.* 2026;83:87-102. DOI PubMed
69. Frangogiannis NG. The fate and role of the pericytes in myocardial diseases. *Eur J Clin Invest.* 2024;54:e14204. DOI PubMed
70. Roth M, Carlsson R, Buizza C, Enström A, Paul G. Pericyte response to ischemic stroke precedes endothelial cell death and blood-brain barrier breakdown. *J Cereb Blood Flow Metab.* 2025;45:617-29. DOI PubMed PMC
71. Zang H, Li X, Yang X, et al. The role of pericytes in homeostasis and cardiovascular disease: a comprehensive review. *J Adv Res.* 2026;88:659-75. DOI PubMed PMC
72. Alarcon-Martinez L, Villafranca-Baughman D, Quintero H, et al. Interpericyte tunnelling nanotubes regulate neurovascular coupling. *Nature.* 2020;585:91-5. DOI PubMed
73. Avolio E, Meloni M, Spencer HL, et al. Combined intramyocardial delivery of human pericytes and cardiac stem cells additively improves the healing of mouse infarcted hearts through stimulation of vascular and muscular repair. *Circ Res.* 2015;116:e81-94. DOI PubMed
74. Tsao CC, Baumann J, Huang SF, et al. Pericyte hypoxia-inducible factor-1 (HIF-1) drives blood-brain barrier disruption and impacts acute ischemic stroke outcome. *Angiogenesis.* 2021;24:823-42. DOI PubMed PMC
75. Yemisci M, Gursoy-Ozdemir Y, Vural A, Can A, Topalkara K, Dalkara T. Pericyte contraction induced by oxidative-nitrative stress impairs capillary reflow despite successful opening of an occluded cerebral artery. *Nat Med.* 2009;15:1031-7. DOI PubMed
76. Gong S, Ma H, Zheng F, et al. Inhibiting YAP in endothelial cells from entering the nucleus attenuates blood-brain barrier damage during ischemia-reperfusion injury. *Front Pharmacol.* 2021;12:777680. DOI PubMed PMC
77. Brock RW, Lawlor DK, Harris KA, Potter RF. Initiation of remote hepatic injury in the rat: interactions between Kupffer cells, tumor necrosis factor-alpha, and microvascular perfusion. *Hepatology.* 1999;30:137-42. DOI PubMed
78. Dominguez JH, Xie D, Kelly KJ. Impaired microvascular circulation in distant organs following renal ischemia. *PLoS One.* 2023;18:e0286543. DOI PubMed PMC
79. Ma Y, Zabell T, Creasy A, et al. Gut ischemia reperfusion injury induces lung inflammation via mesenteric lymph-mediated neutrophil activation. *Front Immunol.* 2020;11:586685. DOI PubMed PMC
80. Uchida K, Mishima S, Ohta SI, Yukioka T. Inhibition of inducible nitric oxide synthase ameliorates lung injury in rats after gut ischemia-reperfusion. *J Trauma.* 2007;63:603-7. DOI PubMed

81. White LE, Santora RJ, Cui Y, Moore FA, Hassoun HT. TNFR1-dependent pulmonary apoptosis during ischemic acute kidney injury. *Am J Physiol Lung Cell Mol Physiol.* 2012;303:L449-59. DOI PubMed PMC
82. Zhu L, Zhou H, Xu F, et al. Hepatic ischemia-reperfusion impairs blood-brain barrier partly due to release of arginase from injured liver. *Front Pharmacol.* 2021;12:724471. DOI PubMed PMC
83. Stagg HW, Bowen KA, Sawant DA, Rodriguez M, Tharakan B, Childs EW. Tumor necrosis factor-related apoptosis-inducing ligand promotes microvascular endothelial cell hyperpermeability through phosphatidylinositol 3-kinase pathway. *Am J Surg.* 2013;205:419-25. DOI PubMed
84. Baoyinna B, He J, Miao J, et al. Activation of USP30 disrupts endothelial cell function and aggravates acute lung injury through regulating the S-adenosylmethionine cycle. *Adv Sci.* 2026;13:e12807. DOI PubMed PMC
85. Gao XM, Su Y, Moore S, et al. Relaxin mitigates microvascular damage and inflammation following cardiac ischemia-reperfusion. *Basic Res Cardiol.* 2019;114:30. DOI PubMed
86. Huang Y, Tan Q, Chen R, Cao B, Li W. Sevoflurane prevents lipopolysaccharide-induced barrier dysfunction in human lung microvascular endothelial cells: Rho-mediated alterations of VE-cadherin. *Biochem Biophys Res Commun.* 2015;468:119-24. DOI PubMed
87. Liu X, Chen X, Zhu Y, Wang K, Wang Y. Effect of magnolol on cerebral injury and blood brain barrier dysfunction induced by ischemia-reperfusion in vivo and in vitro. *Metab Brain Dis.* 2017;32:1109-18. DOI PubMed
88. Shi C, Zhou Y, Zhang Q, Jin W, Dong H. Impaired meningeal lymphatic drainage aggravates LPS-induced neuroinflammation and depression-like behaviors in mice. *Mediators Inflamm.* 2025;2025:4288671. DOI PubMed PMC
89. Chappell D, Jacob M, Hofmann-Kiefer K, et al. Hydrocortisone preserves the vascular barrier by protecting the endothelial glycocalyx. *Anesthesiology.* 2007;107:776-84. DOI PubMed
90. Konijnenberg LSF, Luiken TTJ, Veltien A, et al. Imatinib attenuates reperfusion injury in a rat model of acute myocardial infarction. *Basic Res Cardiol.* 2023;118:2. DOI PubMed PMC
91. Nitzsche A, Poittevin M, Benarab A, et al. Endothelial $S1P_1$ signaling counteracts infarct expansion in ischemic stroke. *Circ Res.* 2021;128:363-82. DOI PubMed PMC
92. Stewart WG, Hejl CD, Guleria RS, Gupta S. Thymosin beta4 stabilizes hypoxia induced brain microvascular endothelial cell dysfunction through S1PR1 dependent mechanisms. *Sci Rep.* 2025;15:45764. DOI PubMed PMC
93. He K, Yan L, Lin SQ, et al. Implication of IGF1R signaling in the protective effect of astragaloside IV on ischemia and reperfusion-induced cardiac microvascular endothelial hyperpermeability. *Phytomedicine.* 2022;100:154045. DOI PubMed
94. Lillo MA, Burboa PC, Durán WN. Active endothelial inactivation of hyperpermeability: the role of nitric oxide-driven cAMP/Epac1 signaling. *J Cardiovasc Dev Dis.* 2025;12:361. DOI PubMed PMC
95. Ge H, Zhu H, Xu N, et al. Increased lung ischemia-reperfusion injury in aquaporin 1-null mice is mediated via decreased hypoxia-inducible factor 2alpha stability. *Am J Respir Cell Mol Biol.* 2016;54:882-91. DOI PubMed
96. Ullah K, Ai L, Li Y, et al. ARNT-dependent HIF-2alpha signaling protects cardiac microvascular barrier integrity and heart function post-myocardial infarction. *Commun Biol.* 2025;8:440. DOI PubMed PMC
97. Patrick R, Pando BD, Yang C, et al. Focal adhesion kinase mediates microvascular leakage and endothelial barrier dysfunction in ischemia-reperfusion injury. *Microvasc Res.* 2025;159:104791. DOI PubMed PMC
98. Huang M, Zhang J, Li M, Cao H, Zhu Q, Yang D. PAK1 contributes to cerebral ischemia/reperfusion injury by regulating the blood-brain barrier integrity. *iScience.* 2023;26:107333. DOI PubMed PMC
99. Jaffer H, Adjei IM, Labhasetwar V. Optical imaging to map blood-brain barrier leakage. *Sci Rep.* 2013;3:3117. DOI PubMed PMC
100. Liang Y, Jiang Y, Liu J, et al. Blood-brain barrier disruption and imaging assessment in stroke. *Transl Stroke Res.* 2025;16:1400-11. DOI PubMed
101. Pham J, Ng FC. Novel advanced imaging techniques for cerebral oedema. *Front Neurol.* 2024;15:1321424. DOI PubMed PMC
102. Sasannia S, Leigh R, Bastani PB, et al. Blood-brain barrier breakdown in brain ischemia: insights from MRI perfusion imaging. *Neurotherapeutics.* 2025;22:e00516. DOI PubMed PMC
103. Zimmerman W, Pergakis M, Ahmad G, et al. Iodine-based dual-energy computed tomography after mechanical thrombectomy predicts secondary neurologic decline from cerebral edema after severe stroke. *Neurocrit Care.* 2025;42:804-16. DOI PubMed
104. Breslin JW, Yuan SY. Determination of solute permeability of microvascular endothelial cell monolayers in vitro. *Methods Mol Biol.* 2024;2711:1-2. DOI PubMed PMC
105. Li Y, Zhou H, Xie J, et al. Targeting TRPV4 to restore glymphatic system function and alleviate cerebral edema in ischemic stroke. *Brain Pathol.* 2025;35:e70022. DOI PubMed PMC
106. van Duinen V, van den Heuvel A, Trietsch SJ, et al. 96 perfusable blood vessels to study vascular permeability in vitro. *Sci Rep.* 2017;7:18071. DOI PubMed PMC

107. Bui Q, Kumar A, Chen Y, et al. CSF-based volumetric imaging biomarkers highlight incidence and risk factors for cerebral edema after ischemic stroke. *Neurocrit Care.* 2024;40:303-13. DOI PubMed PMC
108. Čivrný J, Tomáš D, Černá M. MRI of cerebral oedema in ischaemic stroke and its current use in routine clinical practice. *Neuroradiology.* 2024;66:305-15. DOI PubMed PMC
109. Dhar R, Chen Y, Hamzehloo A, et al. Reduction in cerebrospinal fluid volume as an early quantitative biomarker of cerebral edema after ischemic stroke. *Stroke.* 2020;51:462-7. DOI PubMed PMC
110. Ibrahim T, Hackl T, Nekolla SG, et al. Acute myocardial infarction: serial cardiac MR imaging shows a decrease in delayed enhancement of the myocardium during the 1st week after reperfusion. *Radiology.* 2010;254:88-97. DOI PubMed
111. Jablonowski R, Engblom H, Kanski M, et al. Contrast-enhanced CMR overestimates early myocardial infarct size: mechanistic insights using ECV measurements on day 1 and day 7. *JACC Cardiovasc Imaging.* 2015;8:1379-89. DOI PubMed
112. Mather AN, Fairbairn TA, Artis NJ, Greenwood JP, Plein S. Timing of cardiovascular MR imaging after acute myocardial infarction: effect on estimates of infarct characteristics and prediction of late ventricular remodeling. *Radiology.* 2011;261:116-26. DOI PubMed PMC
113. Xu Z, Zhu Q, Wang LV. In vivo photoacoustic tomography of mouse cerebral edema induced by cold injury. *J Biomed Opt.* 2011;16:066020. DOI PubMed PMC
114. Ding N, Xiang B, Jiang H, et al. OCT-PAM dual-mode imaging to evaluate early ischemic stroke in rats. *J Cereb Blood Flow Metab.* 2026;46:36-50. DOI PubMed PMC
115. Ibrahim T, Nekolla SG, Hörnke M, et al. Quantitative measurement of infarct size by contrast-enhanced magnetic resonance imaging early after acute myocardial infarction: comparison with single-photon emission tomography using Tc^{99m}-sestamibi. *J Am Coll Cardiol.* 2005;45:544-52. DOI PubMed
116. Fuernau G, Eitel I, Franke V, et al. Myocardium at risk in ST-segment elevation myocardial infarction comparison of T2-weighted edema imaging with the MR-assessed endocardial surface area and validation against angiographic scoring. *JACC Cardiovasc Imaging.* 2011;4:967-76. DOI PubMed
117. Ganame J, Messalli G, Dymarkowski S, et al. Impact of myocardial haemorrhage on left ventricular function and remodelling in patients with reperfused acute myocardial infarction. *Eur Heart J.* 2009;30:1440-9. DOI PubMed
118. Ndrepepa G, Tiroch K, Fusaro M, et al. 5-year prognostic value of no-reflow phenomenon after percutaneous coronary intervention in patients with acute myocardial infarction. *J Am Coll Cardiol.* 2010;55:2383-9. DOI PubMed
119. Li W, Hu W, Yuan S, et al. Enhancing blood-brain barrier integrity in patients with acute ischemic stroke via normobaric hyperoxia. *J Am Heart Assoc.* 2024;13:e036474. DOI PubMed PMC
120. Kastrup A, Gröschel K, Ringer TM, et al. Early disruption of the blood-brain barrier after thrombolytic therapy predicts hemorrhage in patients with acute stroke. *Stroke.* 2008;39:2385-7. DOI PubMed
121. Shi ZS, Duckwiler GR, Jahan R, et al. Early blood-brain barrier disruption after mechanical thrombectomy in acute ischemic stroke. *J Neuroimaging.* 2018;28:283-8. DOI PubMed
122. Nägele FL, Scheldeman L, Wouters A, et al. Blood-brain barrier leakage in the penumbra is associated with infarction on follow-up imaging in acute ischemic stroke. *Stroke.* 2025;56:1832-42. DOI PubMed PMC
123. Ye J, Bi X, Deng S, et al. Hypoxanthine is a metabolic biomarker for inducing GSDME-dependent pyroptosis of endothelial cells during ischemic stroke. *Theranostics.* 2024;14:6071-87. DOI PubMed PMC
124. Lee J, Giannaris PS, Yilmaz CE, Yilmaz G. Emerging biomarkers in ischemic stroke. *Vessel Plus.* 2025;9:11. DOI PubMed PMC
125. Qiao Y, Ter Schiphorst A, Xu Y, Baron JC, Zhao W. Revisiting incomplete tissue-level reperfusion following successful thrombectomy for acute ischemic stroke. *Ann Neurol.* 2026;99:668-83. DOI PubMed PMC
126. Li Y, Yao Y, Li J, Chen Q, Zhang L, Wang QK. Losartan protects against myocardial ischemia and reperfusion injury via vascular integrity preservation. *FASEB J.* 2019;33:8555-64. DOI PubMed
127. Ma XX, Xie HY, Hou PP, Wang XJ, Zhou W, Wang ZH. Nuclear factor erythroid 2-related factor 2 is essential for low-normobaric oxygen treatment-mediated blood-brain barrier protection following ischemic stroke. *Mol Neurobiol.* 2024;61:2938-48. DOI PubMed
128. Zhang H, Kim H, Park BW, et al. CU06-1004 enhances vascular integrity and improves cardiac remodeling by suppressing edema and inflammation in myocardial ischemia-reperfusion injury. *Exp Mol Med.* 2022;54:23-34. DOI PubMed PMC
129. Imai T, Matsubara H, Nakamura S, Hara H, Shimazawa M. The mitochondria-targeted peptide, Bendavia, attenuated ischemia/reperfusion-induced stroke damage. *Neuroscience.* 2020;443:110-9. DOI PubMed
130. Shi ZF, Fang Q, Chen Y, et al. Methylene blue ameliorates brain edema in rats with experimental ischemic stroke via inhibiting aquaporin 4 expression. *Acta Pharmacol Sin.* 2021;42:382-92. DOI PubMed PMC
131. Rutkovskiy A, Valen G, Vaage J. Cardiac aquaporins. *Basic Res Cardiol.* 2013;108:393. DOI PubMed
132. Zhang S, Zhao J, Sha WM, et al. Inhibition of EphA4 reduces vasogenic edema after experimental stroke in mice by protecting the blood-brain barrier integrity. *J Cereb Blood Flow Metab.* 2024;44:419-33. DOI PubMed PMC

133. Bao L, Xu Y, Ren Y, et al. The role of ROCK1/MLC/NMMHC IIA-actin signaling in ischemic stroke-induced blood-brain barrier disruption: implications for therapeutic intervention. *Cell Mol Life Sci.* 2025;82:373. DOI PubMed PMC
134. Cai C, Guo Z, Chang X, et al. Empagliflozin attenuates cardiac microvascular ischemia/reperfusion through activating the AMPKalpha1/ULK1/FUNDC1/mitophagy pathway. *Redox Biol.* 2022;52:102288. DOI PubMed PMC
135. Wang T, Liu C, Pan LH, et al. Inhibition of p38 MAPK mitigates lung ischemia reperfusion injury by reducing blood-air barrier hyperpermeability. *Front Pharmacol.* 2020;11:569251. DOI PubMed PMC
136. Kawana S, Okazaki M, Sakaue T, et al. Loss of Nr4a1 ameliorates endothelial cell injury and vascular leakage in lung transplantation from circulatory-death donor. *J Heart Lung Transplant.* 2025;44:249-60. DOI PubMed
137. Cen M, Ouyang W, Zhang W, et al. MitoQ protects against hyperpermeability of endothelium barrier in acute lung injury via a Nrf2-dependent mechanism. *Redox Biol.* 2021;41:101936. DOI PubMed PMC
138. Dasgupta I, McCollum D. Control of cellular responses to mechanical cues through YAP/TAZ regulation. *J Biol Chem.* 2019;294:17693-706. DOI PubMed PMC
139. Wen R, Wang H, Pan W, Yan Z, Wang S. The Piezo1/YAP mechanotransduction axis: from mechanistic insights to therapeutic perspectives in disease. *Biochem Pharmacol.* 2026;253:118290. DOI PubMed
140. Liu X, Luo J, Chen J, et al. The neuroprotection of 1,2,4-triazole derivative by inhibiting inflammation and protecting BBB integrity in acute ischemic stroke. *CNS Neurosci Ther.* 2024;30:e70113. DOI PubMed PMC
141. Zhu L, Huang R, Feng JR, et al. Shexiang Tongxin Dropping Pills attenuate ischemic microvascular dysfunction via suppressing P66Shc-mediated mitochondrial respiration deficits. *J Ethnopharmacol.* 2025;346:119664. DOI PubMed
142. Hu Y, Zheng Y, Wang T, Jiao L, Luo Y. VEGF, a key factor for blood brain barrier injury after cerebral ischemic stroke. *Aging Dis.* 2022;13:647-54. DOI PubMed PMC
143. Zhang H, Park JH, Maharjan S, et al. Sac-1004, a vascular leakage blocker, reduces cerebral ischemia-reperfusion injury by suppressing blood-brain barrier disruption and inflammation. *J Neuroinflammation.* 2017;14:122. DOI PubMed PMC
144. Jiang QY, Qin W, Zhuang JK, et al. MicroRNA-383-5p regulation of NADPH oxidase 4 alleviates hemorrhagic transformation and improves acute outcomes after endovascular recanalization in acute ischemic stroke. *Front Immunol.* 2026;17:1870493. DOI PubMed PMC
145. Arkelius K, Wendt TS, Andersson H, et al. LOX-1 and MMP-9 inhibition attenuates the detrimental effects of delayed rt-PA therapy and improves outcomes after acute ischemic stroke. *Circ Res.* 2024;134:954-69. DOI PubMed
146. Song Y, Wang L, Peng T, et al. Brain-targeting biomimetic nanozyme enhances neuroprotection in ischemic stroke by remodeling the neurovascular unit. *J Control Release.* 2025;382:113750. DOI PubMed
147. Enzmann G, Kargaran S, Engelhardt B. Ischemia-reperfusion injury in stroke: impact of the brain barriers and brain immune privilege on neutrophil function. *Ther Adv Neurol Disord.* 2018;11:1756286418794184. DOI PubMed PMC
148. Sun J, Huang Y, Gong J, et al. Transplantation of hPSC-derived pericyte-like cells promotes functional recovery in ischemic stroke mice. *Nat Commun.* 2020;11:5196. DOI PubMed PMC
149. Zhang M, Kim Y, Bosworth A, et al. Brain pericytes derived from human pluripotent stem cells retain vascular and phagocytic functions under hypoxia. *Stem Cells.* 2025;43:sxaf055. DOI PubMed PMC
150. Dave KM, Stolz DB, Manickam DS. Delivery of mitochondria-containing extracellular vesicles to the BBB for ischemic stroke therapy. *Expert Opin Drug Deliv.* 2023;20:1769-88. DOI PubMed

Disclaimer/Publisher's Note: All statements, opinions, and data contained in this publication are solely those of the individual author(s) and contributor(s) and do not necessarily reflect those of OAE and/or the editor(s). OAE and/or the editor(s) disclaim any responsibility for harm to persons or property resulting from the use of any ideas, methods, instructions, or products mentioned in the content.

© The Author(s) 2026. Open Access This article is licensed under a Creative Commons Attribution 4.0 International License (https://creativecommons.org/licenses/by/4.0/), which permits unrestricted use, sharing, adaptation, distribution and reproduction in any medium or format, for any purpose, even commercially, as long as you give appropriate credit to the original author(s) and the source, provide a link to the Creative Commons license, and indicate if changes were made.